PUBLISHER :

Address of Publisher & Editor's Office :

GDAŃSK UNIVERSITY
OF TECHNOLOGY
Faculty
of Ocean Engineering
& Ship Technology

ul. Narutowicza 11/12
80-952 Gdańsk, POLAND
tel.: +48 58 347 17 93
fax : +48 58 341 47 12
e-mail : sekoce@pg.gda.pl

Account number :
BANK ZACHODNI WBK S.A.
I Oddział w Gdańsku
41 1090 1098 0000 0000 0901 5569

Editorial Staff :
Witold Kirkor Editor in Chief
e-mail : kirwik@interia.pl
Przemysław Wierzchowski Scientific Editor
e-mail : e.wierzchowski@chello.pl
Maciej Pawłowski Editor for review matters
e-mail : mpawlow@pg.gda.pl
Tadeusz Borzęcki Editor for international relations
e-mail : tadbor@pg.gda.pl
Cezary Spigarski Computer Design
e-mail : biuro@oficynamorska.pl

Domestic price :
single issue : 20 zł

Prices for abroad :
single issue :
- in Europe EURO 15
- overseas US$ 20

ISSN 1233-2585

POLISH MARITIME RESEARCH

in internet

www.bg.pg.gda.pl/pmr.html

Index and abstracts of the papers 1994 ÷ 2004

POLISH MARITIME RESEARCH

No 3(45) 2005 Vol 12

CONTENTS

The papers published in this issue have been reviewed by :
Prof. J. Kolenda ; Assoc.Prof. A. S. Lenart
Prof. K. Rosochowicz ; Prof. K. Wierzcholski

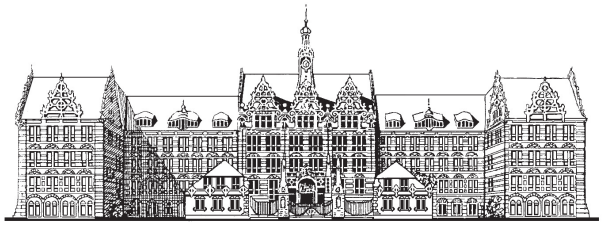

1904 1945 2004/2005

JUBILEE ACADEMIC YEAR 2004/2005
60 YEARS OF GDAŃSK UNIVERSITY OF TECHNOLOGY

Editorial

POLISH MARITIME RESEARCH is a scientific journal of worldwide circulation. The journal appears as a quarterly four times a year. The first issue of it was published in September 1994. Its main aim is to present original, innovative scientific ideas and Research & Development achievements in the field of :

Engineering, **Computing & Technology**, **Mechanical Engineering**,

which could find applications in the broad domain of maritime economy. Hence there are published papers which concern methods of the designing, manufacturing and operating processes of such technical objects and devices as : ships, port equipment, ocean engineering units, underwater vehicles and equipment as well as harbour facilities, with accounting for marine environment protection.
The Editors of POLISH MARITIME RESEARCH make also efforts to present problems dealing with education of engineers and scientific and teaching personnel. As a rule, the basic papers are supplemented by information on conferences , important scientific events as well as cooperation in carrying out international scientific research projects.

Editorial Board

Stability of free-floating ship

Part II

Maciej Pawłowski
Gdańsk University of Technology

ABSTRACT

This is the second part of the paper published in Polish Maritime Research no. 2/2005, dealing with the calculation problem of righting arms of the free-floating ship, i.e. longitudinally balanced at any heel angle. In such case the righting arms are ambiguous as they depend on a way the heeling moment acts. Two cases were considered : when the heeling moment is parallel to the ship plane of symmetry, and the case when it performs the least work, i.e. when the moment is parallel to the main axis of ship waterline. It was demonstrated that angular translations (heel and trim) are then the Euler angles associated with a relevant reference axis. Some cases of the incorrect defining and using of those angles in today design practice were indicated. The most important features of the curve of righting arms of free-floating ship were demonstrated.

Keywords : stability, free floating ship

FEATURES OF RIGHTING ARM CURVE

Knowing metacentric radii of a free-floating ship one can easily find the remaining characteristics of its curve of righting arms. They are analogous to those known from the classical theory of ships.

Hence, the metacentric height h is equal to :

$$h = {}^{d}/_{d\phi}\, GZ = BM - BZ \tag{25}$$

where :

BM - metacentric height according to Eq. (12)
$BZ = -\mathbf{r}\cdot\mathbf{n}$ - height of ship centre of gravity over its centre of buoyancy (Fig. 2)
$\mathbf{r} = \mathbf{GB}$ - radius-vector of ship centre of buoyancy relative to its centre of gravity, and
$\mathbf{n}$ - versor normal to ship waterline according to Eq.(6) or (20).

Eq. (25) can be obtained immediately by considering the buoyancy action line in the rotation plane (Fig.6) for the heel angle increased by $d\phi$. The metacentric height can be also obtained by differentiating the righting arm GZ, acc. to Eq.(10), respective to the heel angle in the ship-fixed reference system.

The derivative is given by the formula :

$$GZ' = \mathbf{e}'\cdot(\mathbf{r}\times\mathbf{n}) + \mathbf{e}\cdot(\mathbf{r}'\times\mathbf{n}) + \mathbf{e}\cdot(\mathbf{r}\times\mathbf{n}') = BM + \mathbf{r}\cdot\mathbf{n}$$

where the sign ['] stands for differentiating respective to ϕ.

It can be demonstrated that the first term equals zero, the second gives the metacentric height BM, and the third is equal to $\mathbf{r}\cdot\mathbf{n}$. Hence the formula is identical with Eq. (25).

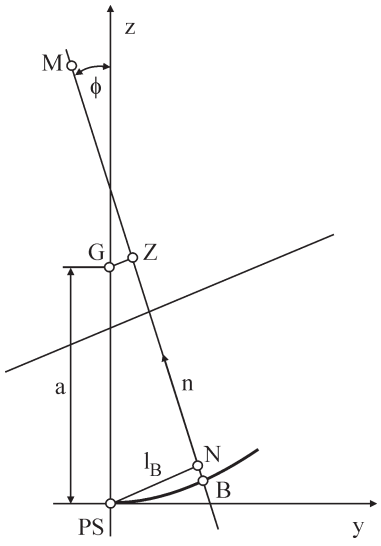

Fig. 6. *Ship rotation plane*

Work done by the heeling moment M is expressed by the formula :

$$L = \int_0^{\phi} M\, d\phi = \Delta \int_0^{\phi} GZ\, d\phi = \Delta l_d \tag{26}$$

where :

Δ - ship buoyancy
l_d - dynamic arm.

It can be observed that the area under the curve of righting arms, called the *dynamic arm*, is proportional to the work of heeling moment.

Considering rotation of the rotation plane (Fig.6) by the angle $d\phi$, one can easily demonstrate that the differential $GZ\,d\phi = d(BZ)$ is an increment of the segment BZ due to vertical translation of the point Z, as the buoyancy centre B translates horizontally relative to ship's waterline. Hence the known formula for the dynamic arm $l_d = BZ - a$, is obtained, where $a = B_0G$ - the height of the gravity centre G over the buoyancy centre of ship in the upright position (i.e. for $\phi = 0$). The equation has simple physical interpretation – the dynamic arm is equal to the vertical increment of the distance between the centre of gravity and centre of buoyancy. It can be useful in checking the calculation accuracy of the righting arm curve.

Worth mentioning that the curve of righting arms of free-floating ship complies with the theorem of minimum potential energy, i.e. ship's heel (understood as a rotation of the plane of rotation) by a given angle demands work done to be minimum. This is an important feature of the curve. To prove it let's observe that to incline the ship from its position of longitudinal equilibrium is not possible without applying a trimming moment and doing an additional work that could increase its potential energy. Hence it results that righting arms of a free-floating ship are at the most equal to or smaller than those of a fixed-trim ship, that is clearly illustrated in Fig.1. If it is not the case, it means that some errors appear in the calculation algorithm.

Cross-curves of stability

The hull form arm, i.e. the arm of buoyancy force relative to the initial location of the centre of buoyancy, shown in Fig.6, is given as follows :

$$l_B = GZ + a\cdot\sin\phi \tag{27}$$

For a free-floating ship which changes its trim during heeling, the hull form arms depend on the height of centre of gravity over BP. Because of trim changes the idea of cross-curves of stability does not apply, strictly speeking, to a free-floating ship. Let's observe that z - axis fixed to the ship does not lie in the rotation plane which is inclined to it by the angle θ. Projection of the axis z to the rotation plane agrees with the axis B_0Z (Fig.6)[4] . Therefore, by shifting the centre of gravity along Oz-axis by the quantity Δz_G it moves before the rotation plane by the distance $\Delta x_2 = \Delta z_G \sin\theta$. As a result the ship becomes unbalanced and it must trim in the vertical plane by the angle $d\alpha_2 = \Delta x_2/BM_L$, where BM_L is the longitudinal metacentric radius at a given heel angle ϕ. The ship can be balanced only by changing its trim, without changing its heel angle. In this case the relationship between both trim angles is the same as in Eq. (23) but without minus sign , i.e. $d\alpha_2 = d\theta\cos\phi$. Hence the trim correction is $d\theta = d\alpha_2/\cos\phi$. From Fig.6 it can be stated that the new righting arm is :

$$GZ_1 = GZ - \Delta z_G\cdot\cos\theta\cdot\sin\phi + (D/\nabla)\, d\alpha_2 \tag{28}$$

where : D - moment of deviation
of ship waterline in $\xi\eta$ - coordinate system (Fig.4).

For normally occurring trim values the function $\cos\theta$ can be omitted as practically being equal to 1. Two first terms of Eq. (28) are the same as for fixed-trim ship. The last term, $(D/\nabla)\, d\alpha_2$, denoted now by Δl, accounts for the effect of trim on the righting arm curve of a free-floating ship. Taking into account that $d\alpha_2 = \Delta x_2/BM_L$, one obtains :

$$\Delta l = \Delta z_G\cdot\sin\theta\cdot tg\chi \tag{29}$$

Hence it can be observed that it is possible to find the righting arm curve for a new location of the centre of gravity by means of cross - curves of stability for free-floating ship provided additional information on the run of the angles θ and χ in function of the heel angle ϕ is available , which makes it possible to calculate the correction Δl. Let's observe that the correction Δl disappears not only when $\theta = 0$, as it could be expected, but also when $\chi = 0$, i.e. when the ship's floatation axis is parallel to the rotation axis. Moreover from Eq. (29) it results that the quotient $\Delta l/\Delta z_G$ is not dependent on a value of changes of the height of centre of gravity over BP; therefore in order to calculate the correction Δl it is enough to know a course of the quotient $\Delta l/\Delta z_G = \sin\theta tg\chi$ in function of the heel angle ϕ. With the use of the quotient, Eq. (28) for the new curve of righting arms obtains the following form :

$$GZ_1 = GZ - \Delta z_G\,(\sin\phi - \Delta l/\Delta z_G) \tag{30}$$

To improve calculation accuracy it is advisable that cross-curves of stability are calculated in the form of the righting arm curves GZ for a selected, typical location of ship's centre of gravity. In such case the correction Δl is small, hence it can be often neglected. Cross-curves of stability are usually presented in the form of the diagram : $GZ = GZ(\nabla, \phi = \text{const})$.

The diagram showing the differential quotient $\Delta l/\Delta z_G = \sin\theta tg\chi$ should be presented in the similar way, in function of the buoyancy ∇, for a fixed ϕ.

OTHER DEGREES OF FREEDOM

In ship hydrostatics in order to describe ship inclination relative to water, are used two mutually indpendent angles which can be interpreted as degrees of freedom, e.g. the analytical angles φ and θ which describe orientation of waterline relative to ship. By using them all other angles between various planes and axes can be expressed.

However the analytical angles are not convenient to describe angular translations of ship's hull. To this end three natural angles (in dynamics called the *Euler angles*) are used. In static problems two angles are sufficient to describe angular translations as any third angle is not necessary due to lack of yaw which means that nodal line orientation is constant in the sea plane. The above discussed angles ϕ and θ associated with Oy-axis and PS (playing the role of plane of nodes) exemplify the Euler angles. As there are two other axes, one can choose degrees of freedom associated with the remaining axes.

For instance, in NAPA software as well as many other computer programs[5] the heel angle is defined as the slope angle of trace of water in stations, relative to Oy - axis, hence it is the angle φ, whereas the trim angle is rotation of the ship around this trace, denoted by θ_x . Hence they are Euler angles associated with x-axis, commonly used in ship dynamics. The nodal line is the trace of water on midship section, fixed in space. The angle θ_x is equal to that of slope of Ox-axis relative to water- level. As $\cos(90° + \theta_x) = \mathbf{i}\cdot\mathbf{n}$, then : $\sin\theta_x = \cos\alpha tg\theta$, or simpler :

$$tg\theta_x = \cos\varphi\cdot tg\theta \tag{31}$$

The versor **n** can be directly expressed by means of the Euler angles. Dividing $\sin\theta_x$ by $tg\theta_x$ one obtains : $\cos\theta_x = \cos\alpha/\cos\varphi$, hence : $n_z = \cos\alpha = \cos\theta_x\cos\varphi$. By substituting them in Eq.(6), the components of the vector **n** take the following form :

$$\mathbf{n} = (-\sin\theta_x\,,\ -\cos\theta_x\cdot\sin\varphi\,,\ \cos\theta_x\cdot\cos\varphi) \tag{32}$$

As $n_y = -\sin\phi$, hence : $\sin\phi = \cos\theta_x\sin\varphi$, from which it results that : $\phi \le \varphi$, which has been already obtained from Eq.(7); both angles are equal to each other in case of no trim. From the

formula for cosα it results that : $\varphi \le \alpha$, hence : $\phi \le \alpha$. The angle $\varphi = \alpha$, in case of no trim or when the heel angle equals 90°.

In the case of the reference axis Oz, the Euler angles are :

- the inclination angle α by which the axis z is deflected from the vertical, given by Eq.(5); it is identical with the slope angle of BP relative to waterline
- as well as the trim angle ψ, i.e. the ship rotation angle around Oz - axis .

The edge of intersection of BP and water level forms a nodal line as its orientation is fixed is space. Both the angles and the nodal line is shown in Fig.3. The angle ψ is equal to the slope angle of trace of water in the plane *z = const* (i.e. nodal line) relative to Ox-axis[6].

This way one obtains as follows :

$$tg\psi = - tg\theta/tg\varphi \qquad (33)$$

From Eqs.(5) and (33) it results that tgα can be taken as a vector composed of tgφ and - tgθ. Hence : $tg\varphi = tg\alpha\cos\psi$, and : $tg\theta = - tg\alpha\sin\psi$. By substituting them in Eq.(6) the components of the vector **n** take the following form :

$$\mathbf{n} = (\sin\psi\cdot\sin\alpha\ ,\ -\cos\psi\cdot\sin\alpha\ ,\ \cos\alpha) \qquad (34)$$

As : $n_y = - \sin\phi$, hence : $\sin\phi = \cos\psi\sin\alpha$, from which it results that: $\phi \le \alpha$; both the angles are equal to each other only in case of no trim.

It is not indifferent which reference axis (and the Euler angles associated with it) is chosen to calculate righting arm curve because location of the rotation plane in which the ship has to be balanced depends on the axis chosen. During balancing the ship, a change of trim angle does not influence the rotation angle.

In the case of Ox reference axis the rotation plane is a vertical section perpendicular to water-level and parallel to water--trace on frame sections (Fig.7); in the case of Oy-axis – it is perpendicular to water-trace on PS (Fig.2), and in the case of Oz-axis – perpendicular to water-trace on BP (Fig.8). In other words, in the case of the reference axis x the rotation plane is *parallel* to nodal line, and in the two latter cases – *perpendicular* to nodal line. The three planes of rotation are not identical which makes that for a free-floating ship righting arms depend on the choice of reference axis. In all the cases the rotation plane is fixed in space, perpendicular to heeling moment vector, vertical, and crossing ship's centre of gravity. The permanent orientation in space is associated with the permanent direction of nodal line in sea-level, due to the lack of yaw. During heeling the buoyancy centre moves along the curve of buoyancy centres located on the rotation plane whose features have been already discussed. For this reason the righting arm curve is a function of the rotation angle of rotation plane, further marked η. In other words, the heel angle of the ship is identical with the rotation angle of the rotation plane.

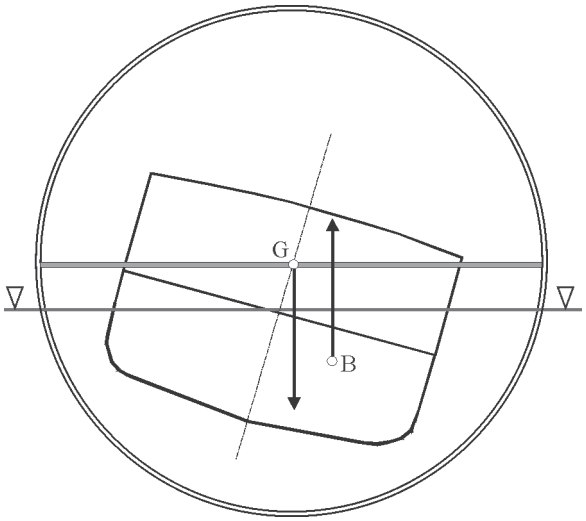

Fig. 7. *Rotation plane of free-floating ship which trims around trace of water on midship section*

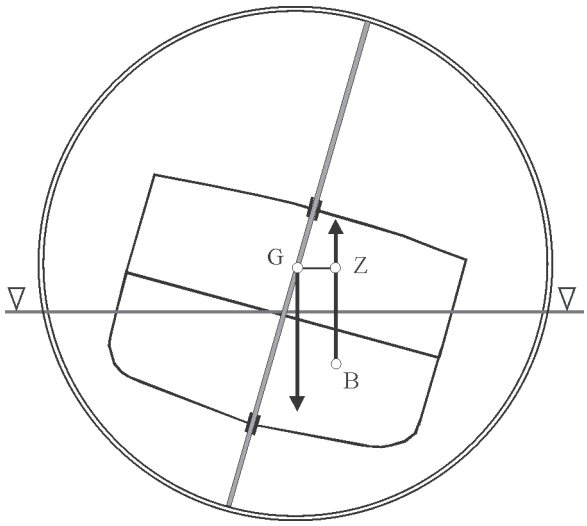

Fig. 8. *Rotation plane of free-floating ship which trims around Oz- axis*

In the case of Ox-axis the rotation angle η cannot be iterpreted simply in geometrical terms. It is also difficult to realize such heeling model physically, that can be observed in Fig.7.

As a result the reference axis is not located in the rotation plane. The rotation angle and heel angle are mutually related by the formula : $d\eta = d\varphi\cos\theta_x$, hence the rotation angle $\eta = \int\cos\theta_x d\varphi$, from which it results that : $\eta < \varphi$, and that for $\varphi = 90°$ the rotation angle of rotation plane is a little smaller than 90° ($\eta < 90°$) .

Generally, differences between the angles η and φ are marginal as $\cos\theta_x$ is practically equal to 1, nevertheless both the angles are not identical. For Oy-axis the rotation angle η is identical with the angle ϕ, and for Oz-axis – with the angle α. In two latter cases shown in Fig.2 and 8, the reference axis is parallel to the rotation plane and it rotates together with the plane.

It can be mathematically demonstrated that the rotation planes associated with particular reference axes are differently situated relative to the ship. To this end it is sufficient to demonstrate that versors normal to the planes, called rotation axes, are different.

When x-axis is a reference axis the vector normal to rotation plane is given by the formula : $\mathbf{e} = \mathbf{e}_2\times\mathbf{n}$, where $\mathbf{e}_2$ – versor of trace of water on frame sections. The versor **e** differs from the versor $\mathbf{e}_1 = (\cos\theta, 0, \sin\theta)$ as for an arbitrarily inclined ship the water-traces on PS and midship section are not mutually normal. As $\mathbf{e}_2 = (0, \cos\varphi, \sin\varphi)$, hence the versor of rotation axis is as follows :

$$\mathbf{e} = (\cos\theta_x\ ,\ -\sin\theta_x\cdot\sin\varphi\ ,\ \sin\theta_x\cdot\cos\varphi) \qquad (35)$$

When Oz- axis is a reference one the versor **e** normal to rotation plane is parallel to the vector : $\mathbf{k}\times\mathbf{n}$. Accounting for that the length of the vector $|\mathbf{k}\times\mathbf{n}| = \sin\alpha$, one obtains as follows :

$$\mathbf{e} = (\cos\psi\ ,\ \sin\psi\ ,\ 0) \qquad (36)$$

which can be directly observed from Fig.3. The versor differs from the two remaining by that it is parallel to BP and waterline – – therefore parallel to common edge of both planes, i.e the

trace of BP on waterline. Let's observe that for $\alpha = 0$ the rotation axis **e** is undefined as the above mentioned planes are parallel and their common edge does not exists; the product $\mathbf{k}\times\mathbf{n}$ is also undefined as both versors are parallel.

As rotation axis in ship's upright position is undefined its choice is arbitrary. It is usually assumed that for $\alpha = 0$ the angle $\psi = 0$, i.e. that in the initial position the rotation axis coincides with the trace of PS on waterline, however not necessarily. As the rotation axis an arbitrary axis on waterline can be chosen, especially its main inertia axis. From the previous considerations on the floatation axis it follows that in the latter case it must permanently coincide with the rotation axis (the angle $\chi = 0$, i.e. $\mathbf{f} = \mathbf{e}$) for every angle of heel Eq. (36) is valid regardless of the choice of rotation axis for $\alpha = 0$ (an axis fixed in space).

The rotation axis is determined by a direction of heeling moment action in a ship-fixed reference system. As for the same analytical angles φ and θ the rotation axes are differently located relative to ship depending on an assumed reference axis, the rotation planes are also different, and hence the righting arms are different. This can be clearly stated from Eq.(10) where the righting arm GZ depends on **r** , **e** and **n**. For the same angles φ and θ, the versor **n** is the same but the rotation planes have different **e** and **r**, which makes GZ arms different. Moreover if in physical space the rotation planes are the same as in Fig.2 , 7 and 8, rotated by the same angle η, then the analytical angles are different, which gives different curves of righting arms in function of the rotation angle η taken as ship's heel angle.

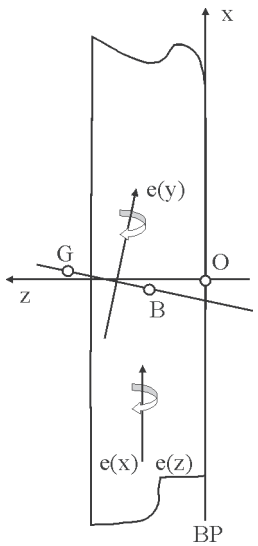

Fig. 9. *Top view of the ship heeled by the angle $\phi = 90°$*

The case of the ship heeled by 90° is interesting as differences between various reference axes can be then distinctly observed. In the case of the reference axis Oy at the angle $\phi = 90°$ PS is horizontal, and the rotation plane crosses ship's gravity centre and buoyancy centre (Fig.9), which means that the ship is longitudinally balanced. As the plane is motionless in space the entire figure should be horizontally rotated around the point G (in this case to the left) by the angle of inclination relative to the axis z. The righting arm is negative and equal to the horizontal distance between the points G and B.

For the axes x and z the rotation planes in Fig.9 cover each other – as they cross the point G parallel to the axis z. As the buoyancy centre is not located on the plane, the ship would so trim (in this case by bow) as to make the centre to be located on the rotation plane.

In both cases the righting arm would be the same, equal to the horizontal distance between the gravity centre and translated buoyancy centre. However the heel angle η, in the sense of the rotation angle of the plane of rotation, would be different. For the axis x the angle η will be less than 90°, even by a few degrees, if trim at large heel angles is significant, which is possible especially in the case of a damaged ship; and for the axis z the angle $\eta = \alpha = 90°$.

The previous considerations dealing with the metacentric radii, floatation axes and curve of righting arms do not lose anything in value if to replace the differential $d\phi$ with the differential $d\eta$, and to substitute η for ϕ . The directed angle $\mathbf{f}d\alpha_1$ is inclined by the angle χ to the appropriate rotation axis **e** defining the axis ξ in Fig.4. The axial component of the angle $d\eta = d\alpha_1\cos\chi$ is the rotation angle of the rotation plane. The component $d\alpha_2$ normal to the rotation axis is given by the formula analogous to Eq. (23) :

$$d\alpha_2 = d\alpha_1\cdot\sin\chi = d\eta\cdot tg\chi = \begin{cases} -\,d\theta_x\text{ , for the reference axis Ox} \\ -\,d\psi\cdot\sin\alpha\text{, for the reference axis Oz} \end{cases} \tag{37}$$

From the above given equation two conclusions analogous to the previous ones, result :

- the more deflected the floatation axis from the rotation axis the greater trim changes during heeling, and
- when $\chi = 0$, i.e. when the floatation axis is parallel to the rotation axis, the ship trim does not change due to rotation of the waterline itself. As opposed to the reference axis Oy, there is no problem with determining the rotation axis at 90° heel for the remaining reference axes.

In the case of the reference axis Ox the rotation axis of the midship section around the normal $\mathbf{i}d\varphi$ has the horizontal component $d\eta = d\varphi\cos\theta_x$ which is axial one. The angle $\mathbf{i}d\varphi$ has also the vertical component equal to $-\,d\varphi\sin\theta_x = -\,d\eta tg\theta_x$.

In the case of the reference axis Oz the vertical component of the rotation angle of BP around the normal $\mathbf{k}d\psi$, equals $d\psi\cos\alpha$. The vertical component makes the angle χ changing by $d\chi_0$ as a result of the change of orientation of rotation axis (relative to the hull), caused by the rotation of the waterline alone. The angle $d\chi_0$ is equal to the vertical component of the rotation. Hence one obtains :

$$d\chi_0 = \begin{cases} -\,d\eta\cdot tg\theta_x\text{ , for the reference axis Ox} \\ -\,d\alpha\cdot tg\chi/tg\alpha\text{ , for the reference axis Oz} \end{cases} \tag{38}$$

In the second part of Eq.(38) the identity appearing in Eq. (37) was utilized. The remaining comments concerning equi-volume waterlines are still valid also for other reference axes. In considerations dealing with cross-curves of stability the angle ϕ should be obviously replaced with a relevant angle η. The quantity $\Delta x_2 = \Delta z_G e_z$, where e_z is z-component of the relevant rotation axis **e**. The differential quotient amounts to :

$$\Delta l/\Delta z_G = e_z tg\chi.$$

RIGHTING ARM CURVE OF MINIMUM STABILITY

As previously mentioned, most heeling moments affecting the ship is parallel to PS, therefore a free - floating ship takes such position relative to its rotation plane as to make trace of water on PS normal to it. Therefore the question arises which position the ship takes when direction of the moment is not associated with its orientation relative to ship's hull. In other words, which reference axis should be then chosen. In order to unambigously answer this question it is necessary to know the mechanism of taking position by the ship relative to its rotation plane in the case of a free-heeling moment.

In the case of a heeling moment not associated with the hull, such, for instance, as that resulting from shifting a weight on ship, or taking a weight to any place on ship, the ship in question rotates in such a way as to make potential energy of the heeled ship minimum [13]. In other words, the ship heels in such a way as the work associated with its heel is minimum. As moment work is proportional to the dynamic arm the minimum value of potential energy corresponds with minimum of the dynamic arm. From the classical ship theory it is known that dynamic arm depends on a course of metacentric radii in function of the heel angle, which – for a free-floating ship – – means : in function of the rotation angle of the rotation plane.

Hence, in general case :

$$l_d = \int_0^{\eta} BM \cdot \sin(\eta - \nu)\, d\nu - a(1 - \cos\eta) \qquad (39)$$

where :

ν - dumb variable of integration, varying from 0 to η (the assumed rotation angle of rotation plane)
BM - metacentric radius given by Eq.(12)
$a = B_0G$ - constant value.

Obviously the integrand in Eq. (39) decides on minimum dynamic arms, which takes its miniumum value for minimum metacentric radii in function of rotation angle. And these appear when instantaneous floatation axis is permanently parallel to the rotation axis (**f** = **e**), i.e. when the angle $\chi = 0$. Hence a free-floating ship under influence of a free-heeling moment takes such position relative to its rotation plane as to make the instantaneous axis of floatation normal to the rotation plane.

A few conclusions yield from that :

- From Eq.(15) it results that the rotation axis coincides – – then and only then – with the floatation axis when the deviation moment D = 0. The floatation axis is then the main inertia axis of the waterplane, for which the transverse inertia moment is minimum. When the ship heel is being changed a new floatation axis rotates relative to the previous one by the angle $d_{\chi f} = d\chi$, which results only from the change of orientation of the main inertia axis of waterline since $d\chi_0 = 0$ due to zero value of the angle χ, which can be deduced from Eq.(38).
- As the floatation axis is permanently parallel to the rotation axis Eq.(11) is reduced to the form : $d\eta = d\alpha_1 = d\alpha$. And, this in turn means that the rotation angle of rotation plane is equal to the angle contained between the actual waterplane and the initial one. Hence the curve of righting arms is a function of the angle α, and Oz - axis is the apropriate reference axis.
- As the angle χ is equal to zero for any angle α the correction Δl takes zero value, which can be seen from Eq. (29). Therefore righting arm curve can be found on the basis of cross-curves of stability by neglecting the correction as in the case of even-keel ship.
- For a given angle α it is necessary to find such value of the angle of rotation around the versor $\mathbf{n}_0$, ψ , as to obtain the centre of buoyancy located in the rotation plane containing the ship centre of gravity, and perpendicular to the longitudinal axis of inertia of waterline.
- Righting arms are then as small as possible and such righting arm curve is called *the curve of minimum stability*. Any other curve can have the same or greater arms.

Worth mentioning that NAPA software as well as many other computer programs used in West countries for ship stability calculations have no possibility to calculate the righting arm curve of minimum stability as such mode of calculations is there unknown at all.

CONCLUSIONS

This paper presents the theoretical background for determining the righting arm curve for a free-floating ship, under assumption that the righting moment has constant direction in space. It is also highlighted what is meant by the heel angle and how ship's longitudinal balance is understood. Results of the performed considerations can be summarized as follows :

- Mode of calculation and choice of a reference axis (Euler angles) considerably influence the results of calculation of the righting arm curve, hence they should be obligatorily defined. Such recommendations are not included in the current rules, which sometimes leads to great discrepances between calculation results obtained from different sources.
- Righting arm curves should be calculated – as a rule – for a free-floating ship balanced in an appropriate rotation plane fixed in space and passing through the ship centre of gravity. The righting arm curve is then a function of the rotation angle of the rotation plane around the normal axis (rotation axis).
- The rotation plane of an *intact* ship is perpendicular to trace of water on PS, being a nodal line,due to the assumed character of heeling moments resulting mainly from horizontal, wind-generated forces. A rotation angle is the slope angle of y-axis relative to water-level, and a trim angle is the slope angle of trace of water on PS relative to BP. They are Euler angles associated with y-axis.
- For a *damaged* ship which mainly heels under influence of vertical forces the rotation plane is perpendicular to the main inertia axis of waterline, being a nodal line. A rotation angle is the angle α contained between the initial waterline and water-level, and a trim angle is the angle contained between trace of water-level and trace of PS on the initial waterline. They are Euler angles associated with the ship-fixed axis normal to the initial waterline. The calculations yield the righting arm curve of minimum stability.
- The notion of cross-curves of stability is valid also for a free-floating ship heeled around the main inertia axis of instantaneous waterline. In other cases the calculated righting arm curve should be corrected by introducing the correction which accounts for an influence of change of trim, resulting from change of height of ship's centre of gravity.
- It is advisable to perform calculations of the righting arm curve by means of the equi-volume waterplane method (Krilov-Dargnies's) which in natural way tracks translation of buoyancy centre during heeling [4]. The method has not been used so far in calculation practice, though it appears not only more accurate and well numerically conditioned, but also it significantly shortens time of calculations (about 20 times) in comparison with bouyancy methods. Therefore it is worth implementing into common practice.

Acknowledgements

The author directs special thanks to Dr Ludwik Balcer of Gdańsk University of Technology for his thorough and critical review of this work, which has greatly raised its educational merits.

NOMENCLTURE

a – height of gravity centre over buoyancy centre in upright position of ship
B – buoyancy centre
BM – transverse metacentric radius
BM_L – longitudinal metacentric radius
BZ – height of gravity centre over buoyancy centre
e – direction of rotation axis (unit vector normal to rotation plane)
$\mathbf{e}_1$, $\mathbf{e}_2$ – versors (unit vectors) of trace of water on PS and on midship plane, respectively
f – versor (unit vector) of floatation axis
F – freeboard
g – gravity acceleration
G – ship gravity centre
GM – metacentric height
GZ – righting arm
i , **j** , **k** – versors (unit vectors) of the ship-fixed reference system whose origin is in the point K (intersection point of the plane of symmetry, PS, midship plane and base plane BP)
l, l_d – righting arm and dynamic arm, respectively
L, B, T – length, breadth and mean draught of ship, respectively
n – upward pointing versor (unit vector) nomal to waterline
∇ – volumetric displacement of ship
α – angle between initial waterline and water-level
β – angle between trace of water on PS and midship plane
Δ – ship buoyancy (weight of displaced water)
Δl – correction of righting arm obtained by means of cross-curves of stability, accounting for oblique translation of gravity centre relative to rotation plane, due to changing the height of ship gravity centre over BP
η – rotation angle of plane of rotation
θ – slope angle of trace of water on PS relative to x-axis of ship
ρ – water density
φ – slope angle of trace of water on the stations relative to y-axis of ship
ϕ – angle of PS inclination from the vertical
χ – angle between floatation axis and rotation axis
ψ – angle between water-level trace line and PS trace line on initial waterline.

Footnotes

4) B_0YZ reference system is fixed to the rotation plane and its origin is located in the initial position of the buoyancy centre B_0.
5) e.g. such as STATAW and SEA software systems used by CTO and PRS.
6) In general case the nodal plane is a plane parallel to waterline of ship in the upright position, which rotates together with it. Its normal versor $\mathbf{n}_0$ is the same as that of initial waterline. The angle α is determined by : $\cos\alpha = \mathbf{n}_0 \cdot \mathbf{n}$, and ψ is the angle between trace of water and trace of PS in nodal plane.

Acronyms

BP – ship's base plane
PS – ship's plane of symmetry
CTO – Ship Design & Research Centre, Gdańsk
PRS – Polish Register of Shipping

BIBLIOGRAPHY

1. Wimalsiri, W. K.: *Design of ro-ro cargo ships with particular reference to damage survivability*. PhD thesis. Dept. of Marine Technology, University of Newcastle upon Tyne. 1991
2. Pawłowski, M.: *On the roll angle for a freely floating rig*. Proceedings of 9th Int. Symposium on Ship Hydromechanics HYDRONAV'91, Gdańsk–Sarnówek. September 1991, Vol. I also in: Budownictwo Okrętowe i Gospodarka Morska, November 1991
3. Pawłowski, M.: *Some inadequacies in the stability rules for floating platforms*. Naval Architect, No. 2, 1992
4. Pawłowski, M.: *Advanced stability calculations for a freely floating rig*. Proceedings of 5th Int. Symposium on Practical Design of Ships and Mobile Units PRADS'92. Newcastle upon Tyne. 1992, Vol. II also in: Report, Dept. of Marine Technology, University of Newcastle upon Tyne. November 1991
5. Kaźmierczak, J.: *Ship floatability and stability* (in Polish). Wydawnictwa Komunikacyjne (Transport Publishing House). Warszawa, 1954
6. Staliński, J.: *Ship theory* (in Polish). Wydawnictwo Morskie (Maritime Publishing House). Gdynia, 1961
7. Rahola, J.: *The judging of the stability of ships and the determination of the minimum amount of stability*. PhD thesis. University of Helsinki. 1939
8. International Maritime Organisation (IMO) : *Recommendation on intact stability criteria for passenger and cargo ships under 100 metres in length*. Resolution A.167 (ES.IV). London, 1987
9. International Maritime Organisation : *Subdivision and damage stability of cargo ships, chapter II–1, part B–1, SOLAS Convention*. Consolidated Edition. 1997
10. Pawłowski, M.: *A closed form assessment of the capsizal probability – the s_i factor*. Proceedings of WEGEMT Workshop on Stability of Ships. Technical University of Denmark (DTU). Lyngby. October 1995
11. Vassalos, D., Pawłowski, M., and Turan, O.: *Criteria for survival in damaged condition*. Proceedings of Int. Seminar on the Safety of ro-ro Passenger Vessels. RINA (Royal Institution of Naval Architects). London. June 1996 also in: *Dynamic stability assessment of damaged passenger ro-ro ships and proposal of rational survival criteria*. Marine Technology, Vol. 34, No. 4, October 1997
12. Huber, M. T.: *Technical stereomechanics (strength of materials)* (in Polish). Ed. II. PWN (State Scientific Publishing House). Warszawa, 1958 also e.g .: Parry, R. H. G.: *Mohr circles, stress paths and geotechnics*. E & FN Spon. London, 1995
13. Siemionov-Tian-Shansky: *Statics and dynamics of ships*. Peace Publishers. Moscow, 1963, also in Russian: *Statika i dinamika korabla*. Sudostrojenie. Leningrad, 1973

CONTACT WITH THE AUTHOR

Maciej Pawłowski, Assoc.Prof.,D.Sc.
Faculty of Ocean Engineering
and Ship Technology,
Gdańsk University of Technology
Narutowicza 11/12
80-952 Gdańsk, POLAND
e-mail : mpawlow@pg.gda.pl

Model test of ship stability (photo: Mirosław Grygorowicz)

A parametric method for preliminary determining of mass characteristics of inland navigation ships

Jan P. Michalski
Gdańsk University of Technology

ABSTRACT

This paper presents a method for estimation of mass characteristics of vessels, elaborated with the use of an algorithm based on requirements of the Rules for the Classification and Construction of Inland Waterways Vessels of Polish Register of Shipping, and on a simplified method [6] for determination of mass of hull plating stiffeners. The dimensioning method of hull structure scantlings based on this algorithm concerns classical vessels intended for the carrying of general cargo, dry and liquid bulk cargoes, which determine the range of the method application. The method does not cover vessels of different construction, e.g. roll-on-roll-off type vessels equipped with heavy decks, as the dimensioning of their scantlings is based on different relationships and models.

Keywords : Inland waterways vessels, ship preliminary design methods

INTRODUCTION

Methods for preliminary, approximate estimation of mass as well as mass centre coordinates of a designed ship is an important branch of ship design theory. Knowledge of the parameters is necessary already in early design phases – to iteratively balance ship's floatability and stability before structural strength calculations are performed.

The subject-matter literature contains some methods concerning this subject, e.g. in [1, 2, 3, 4] and [5], which, however, deal with sea-going ships whose features are different from those of inland waterways vessels. The methods applicable to inland waterways vessels are rather scarce, e.g. [6, 7, 8, 9, 10].

In the preliminary design stage, ship mass and its centre of gravity are usually estimated by means of the methods making use of parent ship's data, if only they are available. In the case when such data are lacking, or if a design project covers a broad range of variability of ship design parameters, e.g. in a design optimization study (with a selected objective function), then use of general parametric methods is necessary to determine ships mass characteristics.

The parametric methods for estimating ship hull mass are elaborated on the basis of either statistical data of existing ships or the rules of classification societies.

A range of applicability of such methods is usually limited by the following factors :

- ship's functional type
- hull structural arrangement
- structural material
- ship's size range.

To elaborate the presented method a set of discrete values of mass of vessel's hull series of systematically varying parameters was simulated by means of the computer implementation [14] of the algorithm [13]. Next, correlations between the hull parameters and their mass characteristics were investigated, which made it possible to reduce some number of unimportant parameters appearing in the problem. Next, analytical relationships approximating the discrete values of mass characteristics were determined. Simulating calculations were carried out for assumed parameters of normal strength (NW) steel – – usually applied for construction of hulls of inland waterways vessels.

The problem is to determine an analytical mathematical model to transform those vessel's features which are known in the preliminary design stage, i.e.

- the numerical parameters of ship $\overline{x} \equiv (L, B, H, T, C_B, ...)$ which describe : main dimensions, hull form, coefficients, structural material properties
- the qualitative atributes $\overline{q} \equiv (K, R, p_1, ..., p_n)$ which identify vessel's functional type, class and topological features of hull structure
- the strength requirements of classification rules ;

into estimated values of the hull mass M and its gravity centre height, Zg :

$$M = F(\overline{x}, \overline{q}) \quad \text{and} \quad Zg = F(\overline{x}, \overline{q}) \tag{1}$$

A practical aspect of this work is to get a parametric method easily codable into a computer program – useful for the estimating of the mass and gravity centre height of inland wa-

terways vessels in the preliminary design stage. The cognitive aspect of the work is to investigate and broaden theoretical knowledge on the relationships between parameters of inland waterways vessels and their mass characteristics.

The research in question has resulted from practical needs which have arisen during studies on the INCOWATRANS E!3065 (Inland and Costal Water Transport System) Project carried out within the frame of the UE EUREKA Program aimed at development of a modern, ecological friendly fleet of inland waterways vessels.

RESEARCH PROGRAM AND ITS ASSUMPTIONS

By making use of relevant knowledge dealing with sea--going ships, given in [5,15] the hull parameters *a priori* assumed to be significantly affecting its mass characteristics, were preliminarily selected. Hull mass magnitude depends on both – – vessel's numerical parameters and its qualitative features. Some assumptions simplifying real relationships were introduced to determine simple mathematical models – describing in an approximate way the problem in question. It was assumed that for purposes of approximate estimation of vessel's mass its hull can be identified enough correctly by the following items :

two functional types of vessel :
dry cargo vessels
liquid cargo vessels

vessel's class
defined by permissible region of navigation

vessel's main particulars :
L - length
B - breadth
H - depth to upper deck
T - design draught
C_B - hull block coefficient

other parameters :
k - permissible stress coefficient
Re - yield strength of structural steel.

The hull structure scantlings of dry cargo vessels and liquid cargo ones are determined in a different way – therefore the following structural elements are taken into account [13] :

for dry cargo vessels :
- hatch openings in decks
- hatch coamings
- specific features of double bottom

for liquid cargo vessels :
- longitudinal bulkheads
- continuous structure of decks
- specific features of double bottom.

Variability ranges of the hull parameters of investigated hull series were determined on the basis of the data from literature [10, 17, 18]. Calculations for hull series covered all combinations of the following items :

- functional types of liquid and dry cargo vessels
- PRS (Polish Register of Shipping) ship classes concerning the restricted navigation regions R : 1, 2, 3
- values of the length L : 25.00 m, 50.00 m, 75.00 m and 100.00 m
- values of the breadth B – resulting from the assumed ratio of L/B : 4, 5, 6
- values of the depth H resulting from the assumed ratio of L/H : 10, 15, 20
- values of the draught T resulting from the assumed ratio of H/T : 1.25, 1.5, 2.0.

Moreover, the following constant parameters were assumed :

- values of the block coefficient C_B : 0.7, 0.8, 0.9
- normal strength (NW) steel of 235 MPa yield strength
- permissible stress coefficient k = 0.7.

The number of hull variants I_w of the hull series is equal to product of variants of values of varying parameters, i.e. : vessel class, length, breadth, depth, draught and block coefficient, namely I_w = 972 variants of hulls of any considered vessel functional type.

Simulating calculations were performed by using the elaborated computer program INLAND_VESSEL_HULL_ _MASS.PAS [14] which realizes the algorithm for determining hull scantlings of inland waterways vessels [13]. Results of the calculations are presented in the report [14].

MODELING VESSEL'S MASS CHARACTERISTICS

An analytical relationship expressing the relation between mass of hull and its main design parameters should have the following features :

- accuracy – to correctly approximate a statistical sample
- simplicity – mathematical model should be convenient for design calculations and computer programming
- good estimating properties – to provide credible predictions.

It is not an easy task to satisfy the above mentioned requirements because of multi-dimensionality and nonlinear character of the analyzed relationships. To find the relations the least square approximation method was applied, and by means of the iterative procedures :

- hypotheses on approximation relationships were stated
- structural parameters of approximation model were determined
- preliminary tests were performed
- approximation hypotheses were verified by assessing measures of accuracy.

To obtain sufficient accuracy a special normalizing technique was applied, similar to that given in [15]. The procedure consisted in preliminary choice of the normalizing function $g(\overline{x})$ monotonically compatible with the approximated function $F(\overline{x})$ – representing discrete values of simulated masses of hull series , and in determining the normalized smooth function $w(\overline{x})$ (of small variations) :

$$\frac{F(\overline{x})}{g(\overline{x})} = w(\overline{x}) \qquad \overline{x} \in \Omega \tag{2}$$

Next, the function $a(\overline{x})$ approximating the normalized function $w(\overline{x})$ is determined. If the determined function $a(\overline{x})$ correctly approximates the function $w(\overline{x})$, then the function $f(\overline{x})$:

$$f(\overline{x}) = g(\overline{x}) \cdot a(\overline{x}) \tag{3}$$

correctly approximates the function $F(\overline{x})$, hence this is the searched for solution of the problem in question.

In the case of modelling hull mass characteristics a normalizing function may be e.g. either the product of vessel main dimensions (modular function) :

$$g(\overline{x}) = L \cdot B \cdot H \tag{4}$$

or the power function :

$$g(\overline{x}) = c \cdot \prod_{i=0}^{n} x_i^{a_i} = c \cdot L^{a1} \cdot B^{a2} \cdot H^{a3} \cdot T^{a4} \cdot C_B{}^{a5} \cdot R^{a6} \quad (5)$$

The proper selection of a normalizing function is important in order to get sufficient accuracy of hull mass characteristics approximation.

APPROXIMATED HULL MASS CHARACTERISTICS

Final results of the best parametric models for mass characteristics are below presented in the tables containing the following items :

- hypothesis on a form of normalizing function
- hypothesis on a form of approximating function with a list of variable parameters (great-letter symbols) and structural constants of the model (small-letter symbols)
- estimated values of structural constants of the mathematical model
- correlation indices for assessing significance of design parameters
- estimated values of approximation accuracy measures, where :
  - E-average [%] – relative percentage error of approximation
  - E-max [%] – maximum relative percentage error of approximation for the whole sample
  - E > x% [%] – percentage of relative errors exceeding x% in the whole sample (of 972 elements).

The requirement for model simplicity was fulfilled by applying the power function formulas only – useful in calculating values of the function derivatives – a feature convenient for linearization of a mathematical model of a design problem.

Hull structure mass estimation

Significance of the influence of vessel parameters on hull structure mass was assessed by means of the determined coefficients of correlation, then non-significant parameters – of small correlation coefficient values – were eliminated from the approximation model. In the case of liquid cargo vessels the obtained best approximation formula is given in Tab.1

Tab. 1. *Structure, constants and accuracy of the approximation formula for hull mass estimation*

Liquid cargo inland vessels – sample of 972 simulated hulls

Approximation hypothesis : $g(\overline{x}) = L \cdot B \cdot H$

$$M_H(\overline{x}) = g(\overline{x}) \cdot f(\overline{x}) = c \cdot L^{cl} \cdot B^{cb} \cdot H^{ch} \cdot T^{ct} \cdot C_B{}^{cc} \cdot R^{cr}$$

Hypothesis verification

Determined values of structural parameters

c	0.0631615	**cl**	1.43625	**cb**	0.973853	**ch**	-0.190530
ct	0.150033	**cc**	0.154456	**cr**	-0.264760		

Correlation coefficients

Variables	**L**	**B**	**H**	**T**	**C_B**	**R**
M_H	0.923	0.938	0.757	0.718	0.017	-0.137

Approximation accuracy measures

E-average [%]	**E-max** [%]	**E > 10%** [%]
3.40	10.08	0.10

In the case of dry cargo vessels the best approximation was obtained by the formula whose description and accuracy assessment is given in Tab.2.

Tab. 2. *Structure, constants and accuracy of the approximation formula for hull mass estimation*

Dry cargo inland vessels – sample of 972 simulated hulls

Approximation hypothesis : $g(\overline{x}) = L \cdot B \cdot H$

$$M_H(\overline{x}) = g(\overline{x}) \cdot (f_1(\overline{x}) + f_2(\overline{x})) = F_1(\overline{x}) + F_2(\overline{x})$$

$$F_1(\overline{x}) = c \cdot L^{cl} \cdot B^{cb} \cdot H^{ch} \cdot T^{ct} \cdot C_B{}^{cc} \cdot R^{cr}$$

$$F_2(\overline{x}) = s \cdot L^{sl} \cdot B^{sb} \cdot H^{sh} \cdot T^{st} \cdot R^{sr}$$

Hypothesis verification

Determined values of structural parameters

c	0.061267634	**cl**	1.701378	**cb**	0.404710	**ch**	0.0183751
ct	0.179208	**cc**	0.163863	**cr**	-0.242087		
s	0.000045058	**sl**	2.06496	**sb**	1.31413	**sh**	1.424301
st	-0.42505	**sc**	----	**sr**	-0.32789		

Correlation coefficients

Variables	**L**	**B**	**H**	**T**	**C_B**	**R**
M_H	0.921	0.897	0.835	0.784	0.006	-0.127

Approximation accuracy measures

E-average [%]	**E-max** [%]	**E > 10%** [%]
3.40	10.08	0.10

Estimation of height of hull structure gravity centre

No correlation was revealed between the gravity centre height and the hull block coefficient C_B as well as the navigation region R – both for dry cargo and liquid cargo vessels.

The best approximation model found for the gravity centre height of liquid cargo vessels, $Zg = f(\overline{x})$, is presented in Tab.3 and in the case of dry cargo vessels – in Tab.4.

Tab. 3. *Structure, constants and accuracy of the approximation formula for hull gravity centre height*

Liquid cargo inland vessels – sample of 972 simulated hulls

Approximation hypothesis : $g(\overline{x}) = H$

$$Zg(\overline{x}) = g(\overline{x}) \cdot f(\overline{x}) = c \cdot L^{cl} \cdot B^{cb} \cdot H^{ch} \cdot T^{ct}$$

Hypothesis verification

Determined values of structural parameters

c	0.46023	**cl**	0.02939	**cb**	1.781E-5	**ch**	0.9250	**ct**	2.753E-5

Correlation coefficients

Variables	**L**	**B**	**H**	**T**	**C_B**	**R**
Z_g	0.826	0.765	1.000	0.932	0.000	0.000

Approximation accuracy measures

E-average [%]	**E-max** [%]	**E > 5%** [%]
0.69	1.59	0.00

Tab. 4. *Structure, constants and accuracy of the approximation formula for hull gravity centre height*

Dry cargo inland vessels – sample of 972 simulated hulls

Approximation hypothesis : $g(\overline{x}) = H$

$$Zg(\overline{x}) = g(\overline{x}) \cdot f(\overline{x}) = c \cdot L^{cl} \cdot B^{cb} \cdot H^{ch} \cdot T^{ct}$$

Hypothesis verification

Determined values of structural parameters

c	0.40144	**cl**	0.09297	**cb**	-1.960E-5	**ch**	0.7177	**ct**	0.000307

Correlation coefficients

Variables	**L**	**B**	**H**	**T**	**C_B**	**R**
Z_g	0.843	0.781	0.998	0.930	0.000	0.000

Approximation accuracy measures

E-average [%]	**E-max** [%]	**E > 5%** [%]
1.64	3.19	0.00

POWER PLANT MASS AND OUTFIT MASS CHARACTERISTICS

Estimation of mass of medium and high-speed marine diesel engines

Ship power plant mass essentially depends on a type of engines of the propulsion system. On inland waterways vessels, are commonly installed medium-speed diesel engines (of 500÷600 rpm) and high-speed ones (of 1500÷1800 rpm), which transfer power either directly, or through mechanical, hydraulic or electrical transmission gear – to the screw propeller(s) of fixed or controllable pitch, often accommodated in a Kort nozzle.

Diesel engine mass depends on its rated torque, power output, cylinder arrangement and its supercharging. Apart from the engine itself, mass of power plant consists of masses of its equipment and systems. Data contained in the subject-matter literature usually concern ship power plants with the engines of low speed – applicable to sea-going ships; e.g. in [1] is given a formula for determining mass of ship diesel engines of low and medium speed – of more than 1000 kW rated power :

$$M_{EN} = 12\left(\frac{P}{n}\right)^{0.84} \quad [t] \qquad (6)$$

where :

P - installed engine power [kW]
n - engine speed [rpm].

Publications dealing with vessel power plants equipped with medium-speed and high-speed diesel engines of relatively small power are scarce.

For purposes of the INCOWATRANS design study on inland waterways passenger vessel, a research work on mass of medium-speed and high-speed engines of small power was performed on the basis of the catalogue data of: Volvo-Penta, Deutz, MAN, Caterpillar, Detroit Diesel, Wola-Henschel and Wärtsilä. The collected data of the engine parameters and its mass values were used as a statistical sample to determine an analytical relationship approximating mass of medium-speed and high-speed marine diesel engines of small power. In result, the following simple formula was obtained :

$$M_{EN} = 7130 \cdot \frac{P^{0.85}}{n^{1.75}} \quad [t] \qquad (7)$$

where :

P - installed engine power [kW]
n - engine speed [rpm]

A comparison of the unit mass of the engines :

$$m_e = \frac{M_{EN}}{P} \ [kg/kW]$$

calculated by the formula (6) – dashed lines (engines for sea-going ships), and (7) – continuous lines (engines for inland waterways vessels) is presented on Fig.1.

From the comparison it results that in the case of medium-speed engines (of 750 rpm) the engine mass according to (7) is greater by about 60% than that estimated by using (6). For the high-speed engines (of 2500 rpm) the mass according to (7) is smaller by about 50% that that estimated by means of (6). For the engines of speeds within the range of 1000÷2000 rpm so estimated values of mass are similar.

Estimation of mass of power plants fitted with medium and high-speed engines

Power plant mass of sea-going ships without stores („dry weight" condition) acc. [1] can be determined as a sum of mass

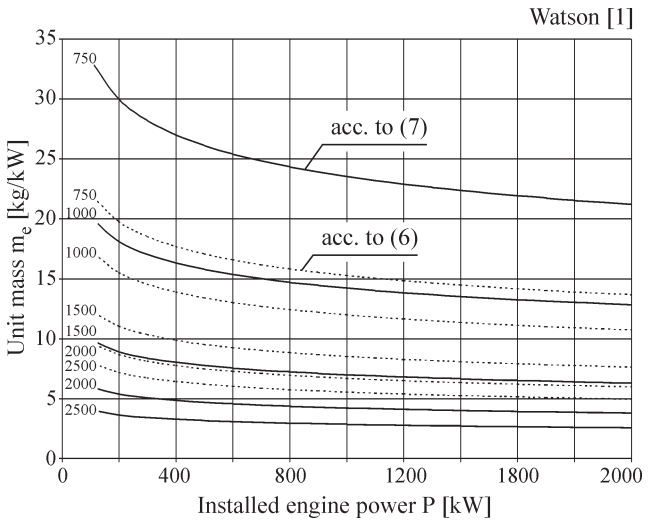

Fig. 1. *Comparison of the values of the unit mass of ship medium- and high-speed diesel engines, obtained from the formula (6) (dashed lines) and (7) (continuous lines)*

of the main engine and mass of the remaining elements of the power plant :

$$M_R = k_R \cdot P^{0.7} \quad [t] \qquad (8)$$

where : k_r - a coefficient taking values from the interval of 0.19 ÷ 0.83 - depending on a ship functional type.

Main engine mass of inland waterways vessels reaches about 30% ÷ 45% of the total mass of the power plant (in "dry weight" condition). To determine mass of a vessel power plant fitted with medium-speed or high-speed engines the following formula was elaborated :

$$M_P = 7130 \cdot \frac{P^{0.85}}{n^{1.75}} + k_R \cdot P^{0.7} \quad [t] \qquad (9)$$

Fig.2. presents a comparison of the unit mass of power plants

$$m_p = \frac{M_P}{P} \ [kg/kW]$$

calculated by means of the formula (6) and (8) – dashed lines, and formula (9) – continuous lines – in both cases $k_R = 0.2$

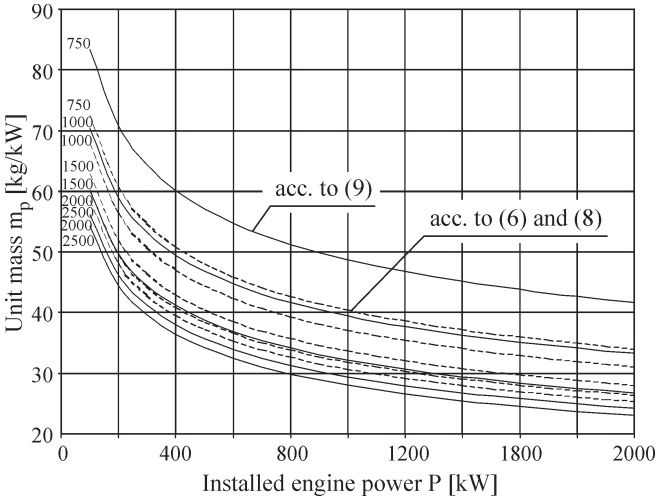

Fig. 2. *Comparison of the unit mass of ship power plants with medium- and high-speed diesel engines, obtained from the formula (6 and 8) – dashed lines, and formula (9) – continuous line*

In the case of power plant of high-speed engines it is often necessary to apply a reduction gear. To estimate mass of

a mechanical reduction gear the following formula was elaborated :

$$M_G = 4 \cdot \frac{P}{n} \quad [t] \qquad (10)$$

Estimation of hull outfit mass

Mass characteristics of hull outfit are not easily modeled mathematically as they depend not only on numerical parameters of a ship but also on such factors as: ship functional type, outfitting standard, crew number, as well as on obligatory requirements of relevant provisions of maritime administration and a society classification rules. Within the frame of the INCOWATRANS project no such research work was made. But on the basis of the diagrams given in [7] the following approximating analytical formula concerning inland waterways vessels, useful in the preliminary design stage, were elaborated :

hull equipment mass :

$$M_E = 0.125 \cdot (L \cdot B \cdot H)^{2/3} \quad [t] \qquad (11)$$

mass of hull systems :

$$M_S = 0.25 \cdot (L \cdot B \cdot H)^{1/2} \quad [t] \qquad (12)$$

hull outfit mass :

$$M_O = 0.025 \cdot (L \cdot B \cdot H)^{2/3} \quad [t] \qquad (13)$$

where all dimensions are in [m].

PRELIMINARY ASSESSMENT OF THE METHOD'S PREDICTING CAPABILITY

An attempt to preliminarily assess predicting capability of the method in question was made by taking into account, as an example, several vessels whose data were obtained from their PRS class documentation. In the case of the SINE 207 inland waterways container vessel of 18/36 TEU capacity its preliminary design documentation was used. Results of the verifying calculations are presented in Tab.5.

SUMMARY

- The scantling determination algorithm used to elaborate the presented parametric method concerns the inland waterways vessels intended for the carrying of general cargo and dry and liquid bulk cargoes.
- The performed verification of the method showed that in the case of the passenger vessels and container vessels the achieved predictions of :
  - ★ mass characteristics – are acceptable approximations for purposes of the preliminary design stage (mean error is of about 15%)
  - ★ gravity centre height characteristics – are acceptable approximations for purpopses of the preliminary design stage (mean error is less than 14%)
- In the case of the vessels of a different structure, e.g. car ferries – intended for the carrying roll-on – roll-off cargoes, fitted with heavy decks (M/V Berlin, M/V Bielik II), the obtained results are different from the values summed up of detail mass specifications.
- For light cargo vessels the proposed parametric method of mass prediction can be a useful tool in preliminary design stage.

NOMENCLATURE

B - breadth
C_B - block coefficient
E - relative percentage error
$f(\overline{x})$ - approximating function of hull mass and its gravity centre
$F(\overline{x})$ - approximated function of hull mass and its gravity centre height
$g(\overline{x})$ - normalizing function
H - depth
L - length
m_e - unit mass of engine
m_p - unit mass of power plant
M_E - hull equipment mass
M_H - hull mass
M_L - real vessel mass

Tab. 5. *Results of verifying calculations to assess predicting capability of the presented method*

Parameters		Vessel name and functional type						
Symbol	Unit	SINE207 *Container*	Berlin *Car ferry*	Arno II *Passenger*	Bielik II *Car ferry*	Bełdany *Passenger*	Perkoz *Passenger*	Posejdon *Passenger*
L	[m]	56.5	51.85	33.58	47.51	33.56	21.4	21.16
B	[m]	9	12.72	6.2	15.59	6.1	4.12	4.23
H	[m]	3.00	6.80	2.96	6.40	2.90	1.5	1.20
T	[m]	1.6	2.74	1.5	2.25	0.94	0.7	0.65
C_B	[-]	0.9	0.55	0.46	0.7	0.6	0.6	0.6
R	[-]	3	3	2	3	3	3	3
P	[kW]	620	820	300	1000	160	70	110
n	[rpm]	1500	500	500	1500	500	1500	1500
M_H	[t]	128.5	153.1	42.6	135.1	36.2	13.5	13.1
M_P	[t]	22.7	62.3	28.0	32.2	17.1	4.6	6.4
M_E	[t]	16.6	34.0	7.6	28.3	5.8	3.2	2.8
M_S	[t]	9.8	16.7	5.4	14.6	4.5	2.9	2.6
M_O	[t]	3.3	6.8	1.5	5.7	1.2	0.6	0.6
M_{LP}	[t]	180.8	273.0	85.2	240.1	71.7	24.9	25.5
M_L	[t]	144.5	734.5	98.7	657.8	85	23.4	20.2
E_M	[%]	20	63	10	64	16	6	21
Z_{gr}	[m]	1.78	4.27	2.10	3.79	2.00	1.07	0.90
Z_g	[m]	1.95	4.08	2.49	3.73	1.83	1.01	1.28
E_Z	[%]	9	5	16	2	8	6	30

M_{LP} - predicted mass of vessel
M_O - hull outfit mass
M_P - power plant mass
M_S - mass of hull systems
n - engine speed
NW - normal strength steel acc. PRS
P - installed (rated) engine power
$\overline{q}$ - vector of qualitative design attributes of vessel
R - permissible region of navigation
T - draught
$\overline{x}$ - vector of numerical design parameters of vessel
Z_g - predicted height of vessel's gravity centre
Z_{gr} - real height of vessel's gravity centre
Ω - set of acceptable parameters.

BIBLIOGRAPHY

1. Watson D.G.M.: *Practical ship design*. Elsevier, 1998
2. Kupras K., Sokołowski K.: *Calculation methods for preliminary ship design (Collection I)* (in Polish). Wydawnictwo Morskie (Maritime Publishing House). Gdynia, 1968
3. Buczkowski L., Bujnicki A., Szymański T., Trafalski W., Wiśniewski J. : *Calculation methods for preliminary ship design (Collection II)* (in Polish). Wydawnictwo Morskie (Maritime Publishing House). Gdańsk, 1976
4. Aszik W.W., Ławkin N.P., Erochowa N.S.: *Rasczet massy korpusa suchogruznych sudow* (in Russian). Sudostroenie No 6/1970
5. Nogid L.M.: *Theory of ship design* (in Polish). Wydawnictwo Morskie (Maritime Publishing House). Gdynia, 1962
6. Kandel F.G., Koszkin E.A., Fridljanskij A.Z.: *Priblizennoje opriedjelenie massy metalliczeskowo korpusa sudow wnutriennewo i smieszanowo pławania* (in Russian). Sudostroenie. No 9/1972
7. Dormidontow N.K., Anfimow W.N., Małyj P.A., Pachomow B.A., Szmujłow N.Ł.*: Projektirowanie sudow wnutriennewo pławania* (in Russian) Izdatielstwo Sudostrojenie. Leningrad, 1974
8. Michalski J.P.: *Assumptions for a calculation program of hull weight and weight centre coordinates of inland navigation pushed barge* (in Polish). Gdańsk University of Technology, Ship Research Institute, Research work report No. 131. Gdańsk, 1969
9. Michalski J.P.: *Description of the calculation program of hull weight and weight centre coordinates of inland navigation pushed barge* (in Polish). Gdańsk University of Technology, Ship Research Institute, Research work report No.133. Gdańsk, 1969
10. Bogdanow B.W., Słuckij A.W., Szmakow M.G.,Wasiliew K.A., Sorkin D.H.: *Buksirnyje suda*.(in Russian). Izdatielstwo „Sudostroenie". Leningrad, 1974
11. Polish Register of Shipping :*Rules for the Classification and Construction of Inland Waterways Ships. Part II : Hull*.(in Polish) 3rd edition. Gdańsk, 2004
12. Polish Register of Shipping :*Rules for the Classification and Construction of Inland Waterways Ships. Part I : Classification Regulations* (in Polish). Gdańsk, 1997
13. Michalski J.P.: *Computer algorithm for determining hull mass and height of its gravity centre of inland navigation ships – verification of the estimated hull mass of SINE 207 ship* (in Polish). Research work report No. 112/E/2004, Faculty of Ocean Engineering and Ship Technology, Gdańsk University of Technology
14. Michalski J.P.: *INLAND_SHIP_HULL_MASS.PAS computer program and complete results of simulating calculations of hull mass of inland navigation ships* (in Polish). Research work report No. 113/E/2004, Faculty of Ocean Engineering and Ship Technology, Gdańsk University of Technology
15. Michalski J.P.: *Calculation methods for determining ship hull resistance and its generalized mass, useful for preliminary design of twin-hull ships of small waterline area* (in Polish). Wydawnictwo Politechniki Gdańskiej, Monografie 24. (Publishing House of Gdańsk University of Technology, Monography 24). Gdańsk, 2002
16. Pacześniak J., Staszewski J.: *Design of sea-going merchant ships , Vol. I and II*. (in Polish). Wydawnictwo Politechniki Gdańskiej (Publishing House of Gdańsk University of Technology). Gdańsk, 1984
17. Kulczyk J., Winter J.: *Inland waterways transport* (in Polish). Oficyna Wydawnicza Politechniki Wrocławskiej (Publishing House of Wrocław University of Technology). Wrocław, 2003
18. Żylicz A.: *Inland navigation ships* (in Polish). Wydawnictwo Morskie (Maritime Publishing House). Gdańsk, 1979

CONTACT WITH THE AUTHOR

Jan P. Michalski, Assoc.Prof.
Faculty of Ocean Engineering
and Ship Technology,
Gdańsk University of Technology
Narutowicza 11/12
80-952 Gdańsk, POLAND
e-mail : janmi@pg.gda.pl

FOREIGN *conference*

上海交通大學
Shanghai Jiao Tong University

Ship Stability Workshop

After the preceding workshops of the kind held in Great Britain, Japan, Greece, Canada, Italy and USA, the 7th International Ship Stability Workshop was organized in China. The interesting scientific meeting of naval architects was held on 1÷3 November 2004 in Shanghai Jiao Tong University.

Its program contained 28 papers
presented during the following sessions :

- Theoretical Development in Damage Stability
- Damage Survivability Assessment
- Assessment of Ship Stability Safety
- Theoretical Prediction of Intact Stability
- Experimental Investigation of Intact Stability
- Ship Dynamics with Water on Deck and Extreme Waves
- Stability Research in China

Authors of the papers represented scientific centres of Canada, China, Finland, Germany, Greece, Holland, Italy, Japan, Sweden, United Kingdom and USA.

Among them it was Prof. M.Pawłowski from Gdańsk University of Technology, Poland, who took part in the activity of International Standing Committee, and – during 2nd session – presented the paper titled :

General framework of new subdivision regulations

Photo : Beata Gis

Design of yacht ports - marinas

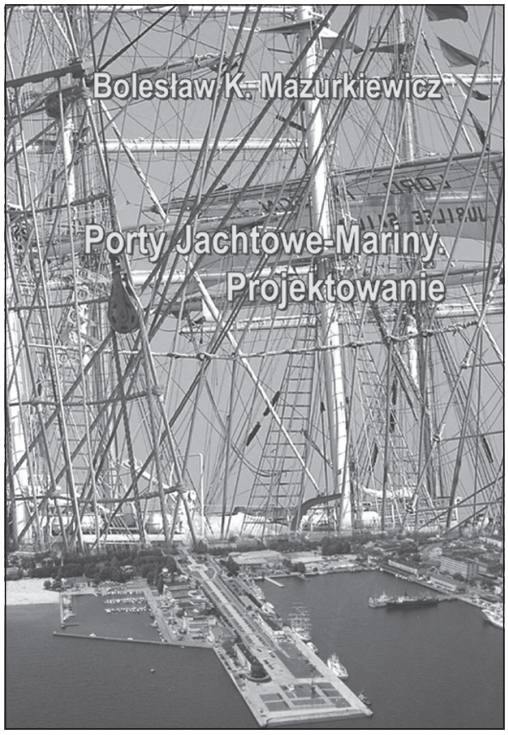

A new handbook written by Prof. B. K. Mazurkiewicz has been recently published (in Polish) by the Foundation for the Promotion of Maritime Industry, Gdańsk.

The book consists of five following chapters :

1. **General information**

This chapter (of 46 pages) contains general information on yachts, definition and classification of yacht ports as well as information dealing with their development in the light of the integrated management of coastal areas. Moreover prospects for building and modernizing yacht ports in Poland are also described.

2. **Location, general arrangement**

In this chapter (of 51 pages) , after presentation of conditions for location of yacht ports, with special attention paid to those demanded by the environment, are presented information and recommendations concerning elaboration of general arrangement and spatial plan of a yacht port - marina. Moreover, parameters of the yacht port - marina as well as of inland waterways and water areas are described in detail.

3. **Solutions of hydro-engineering structures of yacht ports - marinas**

This chapter, the largest (of 136 pages) is devoted to the designing and construction of different hydro-engineering harbour structures such as breakwaters, quays, fixed and floating platforms, mooring posts as well as locks and slipways. Especially great attention is payed to the breakwaters and floating platforms, and first of all to anchoring such structures. There are also given calculation methods mainly for floating platforms more and more frequently used in yacht ports - marinas. Due to the presented broad information on different floating platforms it is possible to make direct use of it in selecting parameters and solutions of the platforms functioning both as mooring ones and pedestrian passages.

4. **Equipment of yacht ports - marinas**

This chapter (of 45 pages) contains information and recommendations concerning devices of different types required for a yacht port - marina. These are : mooring devices and fenders, electrical installations, water supply, fire--fighting and telecommunication systems, devices and installations for receiving, collecting and carrying away waste and sewage, fuel supply stations for yachts, facilities for hoisting, transporting and launching floating units being repaired or stored (wintering) in a given port as well as facilities making it possible to properly manage a yacht port -- marina and to ensure safety to floating units lying in it. To it belongs also navigation marking which makes it possible to safely reach an accomodation or repair berth. Summing up, the chapter covers the main requirements for design and use of different facilities and equipment necessary in a modern yacht port - marina.

5. **Design of yacht port - marina**

In the 5th chapter (of 15 pages) is presented the scope of design of yacht port - marina with drawing attention to an appropriate sequence of design tasks to be elaborated, with reference given to particular chapters of the book. It is assumed that elaboration of design of a yacht port - marina on the basis of the proposed scope and course of designing would allow to avoid mistakes which usually demonstrate as late as during operation of a yacht port - marina. The chapter is illustrated by selected designs of yacht ports -- marinas.

At the end of the book the used nomenclature and referred to bibliography (containing 81 items) is attached.

Yacht port - marina in Łeba (photo: C. Spigarski)

Experimental values of temperature distribution in a sliding bearing sleeve lubricated with non-Newtonian oils

Andrzej Miszczak
Gdynia Maritime University

ABSTRACT

This paper presents results of experimental investigations of temperature distributions on inner surface of a sleeve of transverse sliding bearing lubricated with non-Newtonian oils. The measurements were performed by means of Pt100 miniature sensors placed close to internal surface of the sleeve. To measure sleeve temperature distributions use was made of a test stand installed at Gdynia Maritime University. Delo® 1000 Marine 30 oil, SAE 15W40 basic oil, and a ferro-oil made of the SAE 15W40 basic oil were used as a lubricating medium. During measuring temperature distributions for the ferro-oil different intensity values of external magnetic field generated by electromagnets were applied.

Key words : ferro-oil, non-Newtonian oil, temperature distribution, test stand

AIM OF MEASUREMENTS AND DESCRIPTION OF TEST STAND

The main aim of the measuring of temperature distribution on the inner surface of the sleeve was to investigate influence of magnetic particles contained in oil as well as of external magnetic field intensity values on temperature distribution in slide bearing.

The experimental investigations was performed on the test stand installed at Gdynia Maritime University. The stand was built with making use of a part of T - 05 tester elaborated by Institute of Operation Technology, Radom (Fig.1.) The stand's design was made on the basis of own observations of this author and other designs presented in [1,2]. In the stand a new shaft with 100 mm diameter of journal was applied. The existing driving motor was replaced with a new one of 2.2 kW output and twice greater rotational speed than original.The SJ100-022 HFE *Hitachi* inverter was applied to made continuous control of rotational speed possible.

The stand in question makes also possible to measure relative eccentricity and friction force at given operational parameters such as : inlet oil pressure, load, rotational speed, temperature of sleeve or oil at inlet [3,4].

To measure friction force a tensometric gauge fitted with KT 1400/K/200N/2410D transducer of *Megatron*, was applied. Its measuring range for friction force reaches 200N at 0.17% non-linearity and 0.1N resolution, which gives 5mV output voltage. The gauge is supplied with 24V constant voltage and an output voltage signal is contained within 0÷10V range, equivalent to measured forces within 0÷200N range.

To determine relative eccentricity, two MDCT2/K/2410 induction extensometers of *Megatron* were added to the stand. The extensometers had built-in transducers which made it possible to read output signal in the form of standard voltage signal of 0÷10V range.

One of the extensometers was installed horizontally, the other – vertically [3,4]. They were of ±1mm range at 1μm resolution, which is equivalent to 5mV output voltage. When the measurements of the maximum sleeve translation to the left and right are made by means of the horizontal extensometer, and next the measurements of the maximum sleeve translation up and down with the use of the vertical one, then from the obtained results a value of the radial clearence of the sleeve, ε, location of the journal centre O and that of the sleeve O' , can be determined both in the hot and cold condition of the test stand. Additionally MDS10P *Technicad* contactless eddy-current sensor of journal's translation was installed to take into account journal's deflection under load.

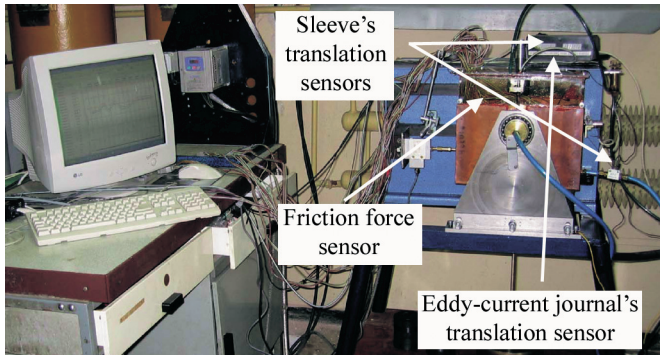

Fig.1. *General view of the test stand for determining temperature distributions, measuring friction force and relative eccentricity in journal sliding bearing*

An additional oil tank fitted with a water cooler and 1 kW electric heater fed from an autotransformator was applied to deliver lubricating oil of appropriate temperature values to the sliding friction node. The delivered oil temperature was so controlled as to maintain it constant at oil inlet. In the lubricating system a PZ3-4/16-1-122 gear pump of 5÷6 l/min capacity and

6 bar maximum pressure, as well as a manometer and a set of control valves, were installed.

The recording of indications of the translation transducers , of friction force transducer and temperature gauge , was performed by means of *Catman* computer software and UPM100 100-channel signal recorder of *Hottinger Baldwin Messtechnik*. With the use of the recorder standard voltage and current signals can be saved, temperature values can be measured by means of thermocouples and resistance gauges, e.g. of Pt100 type, as well as indications of tensometers can be measured.

A DC-supplied electromagnet (Fig.2) was built to investigate magnetic field influence on operational parameters and temperature distribution within the gap of the sliding bearing lubricated with ferro-oil. The maximum value of the magnetic field generated by the magnet was 100 mT. The magnetic saturation of the waste ferro-oil was 50÷70 mT. Magnetic field values were measured with the use of a SMS-102 magnetic field meter fitted with a transverse sound, produced by *Asonik*.

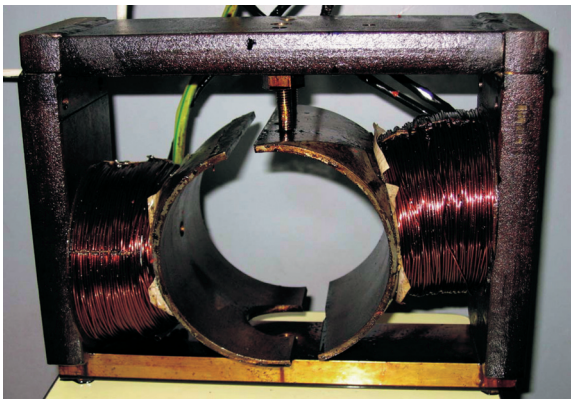

Fig. 2. *General view of the applied electromagnet*

BEARING MATERIALS

To determine temperature distribution over sleeve's inner surface the sliding sleeve made of PBM 100120120 bronze by SKF, having the following dimensions : 100 mm inner diameter, 120 mm outer diameter and 120 mm length, was selected. In the sleeve several holes to accommodate Pt100 gauges in accordance with Fig.3 were made. The gauges were placed 0.5 mm deep above the inner surface of the sliding sleeve. A way of measuring the temperature distribution was assumed the same as in the work [5]. Contact between a gauge and sleeve was improved by covering the gauge with a heat-conducting paste. The gauges were poured with an epoxy resin and connected with the UPM100 recorder by means of conductors. Fig.4 presents the arrangement of the gauges in the sleeve.

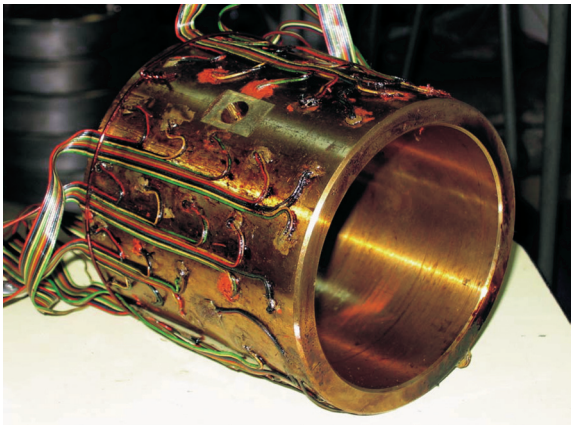

Fig. 4. *General view of the sliding sleeve for measuring temperature distribution and heat flux density*

Temperature distribution measurements were carried out for strictly determined operational parameters of the bearing and the following grades of engine oil applied as a lubricating medium :

- Delo® 1000 Marine 30 *TEXACO* ship engine oil – in fresh condition
- the same Delo® 1000 Marine 30 – in a waste condition, i.e. after 300 h continuous operation within a ship engine (of an oil-rig support & salvage tug); the oil change time recommended by ship's owner was 300 h
- Ferro-oil – made by *FerroTec* on the basis of SAE 15W40 mineral oil free of any bettering additives (i.e. basic oil). In the oil were contained Fe_3O_4 magnetic particles of 5÷15 nm in size and amount of abt. 1.5% vol., as well as a surface-active substance to prevent magnetic particles against clustering
- SAE 15W40 basic oil – delivered by Gdańsk Oil Refinery for testing

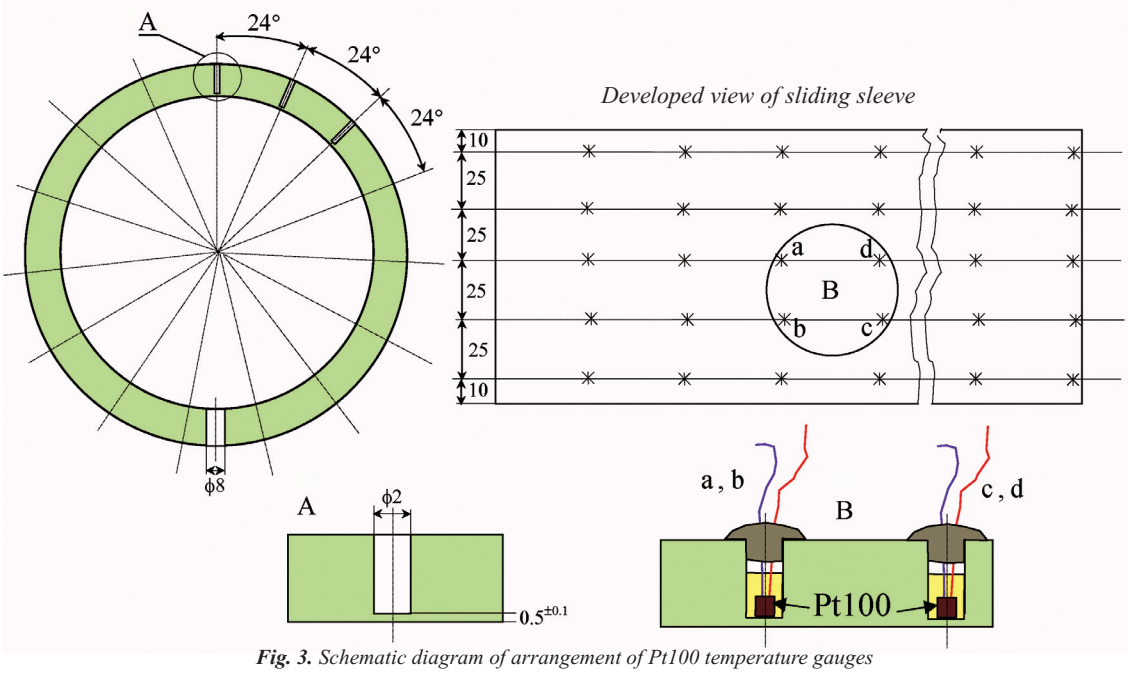

Fig. 3. *Schematic diagram of arrangement of Pt100 temperature gauges*

TEMPERATURE DISTRIBUTION MEASUREMENTS

Due to different properties of the tested oils as well as to be able to determine differences in results of measured temperatures, all the tested oils were subjected to the same selected operational parameters of the bearing. It was : its rotational speed, load, inlet pressure and temperature of lubricating oil. Tab.1. presents values of the operational parameters applied during measurements of temperature distribution.

Tab.1. *Values of operational parameters of tested bearing*

Load [N]	**Inlet oil pressure** [bar]				
	2	1.5			1
	Rotational speed [rpm]				
1034.7	2800	840	1960	2800	2800
2020	2800	840	1960	2800	2800
	Inlet oil temperature : 70°C				

The measured radial clearance ε of the tested bearing was 0.081 mm, which corresponded with the relative radial clearance ψ = 0.0016.

Before the measurements the test stand was thermally stabilized by keeping a high speed of the journal for abt.1h at simultaneous loading the sleeve with a weight. After such operation performed in each case, appropriate values of the operational parameters were set, some time was waited till stabilization of temperature indications takes place, and next the relevant temperature distribution measurements carried out.

In this paper only some results selected out of a broad testing program are presented in the form of diagrams of measured temperature distributions.

Results for Delo® 1000 Marine 30 oil in fresh condition

In Fig.5. are presented measured values of temperature distribution over the surface of PBM 100120120 sleeve for Delo® 1000 Marine 30 oil in fresh condition, under 1034.7N load, at 1.5 bar pressure and its 70°C temperature of oil at inlet, as well as for three following rotational speeds : 840 rpm (Fig.5a); 1960 rpm (Fig.5b); 2800 rpm (Fig.5c). In every figure are presented the same two temperature distributions, but shown in a different axonometric view.

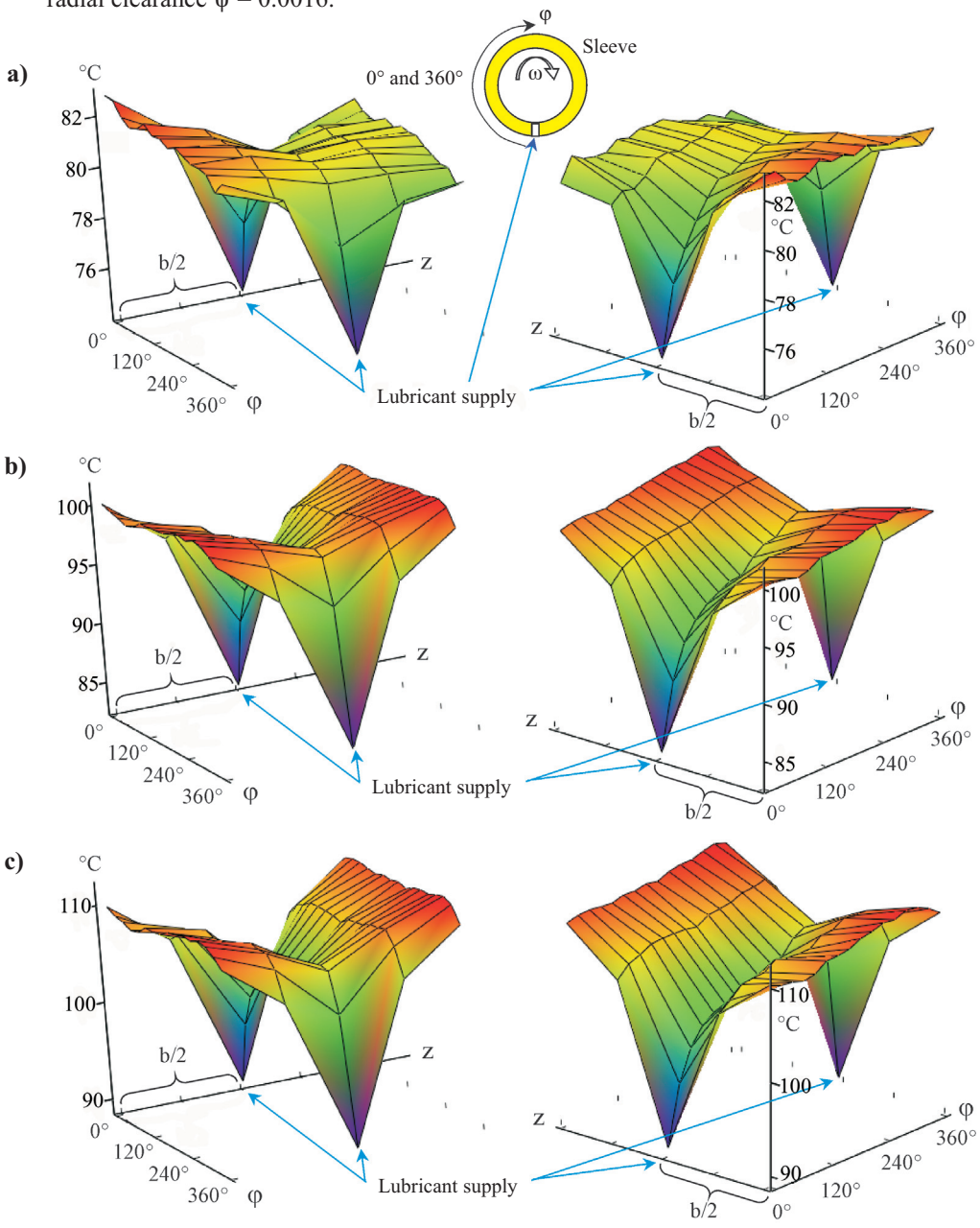

Fig. 5. *Distributions of the temperature measured on the sleeve under 1034.7 N load at 1.5 bar pressure and 70°C temperature of oil at inlet, and the following values of journal's rotational speed :* ***a)*** *840 rpm;* ***b)*** *1960 rpm;* ***c)*** *2800 rpm*

In all the diagrams, φ axes describe the direction of bearing angle, beginning from the point of some degrees behind the point of lubricating oil delivery, towards shaft's rotation. The second horizontal axis marked *z* points along bearing's length (b = 120 mm). In the middle length of the bearing a hole is made through which lubricating oil is delivered. The sleeve was not fitted with distinct oil pockets, but only with a small circular cavity abt. 0.8 mm deep, and of 10 mm diameter.

In Fig.6. is presented the influence of inlet pressure values on temperature distribution in the same oil at only one rotational speed of the journal but two values of inlet oil pressure.

Fig.6a shows the temperature distribution measured on the inner surface of the sleeve at 1 bar inlet oil pressure, under 1034.7 N load, and 70°C inlet oil temperature, and 2800 rpm rotational speed of the journal. Fig.6b shows the temperature distribution for the same values of operational parameters of the bearing as for the Fig.6a, but for the different value of inlet oil pressure, equal to 2 bar. The temperature distributions for 1.5 bar oil pressure are shown in Fig.5c.

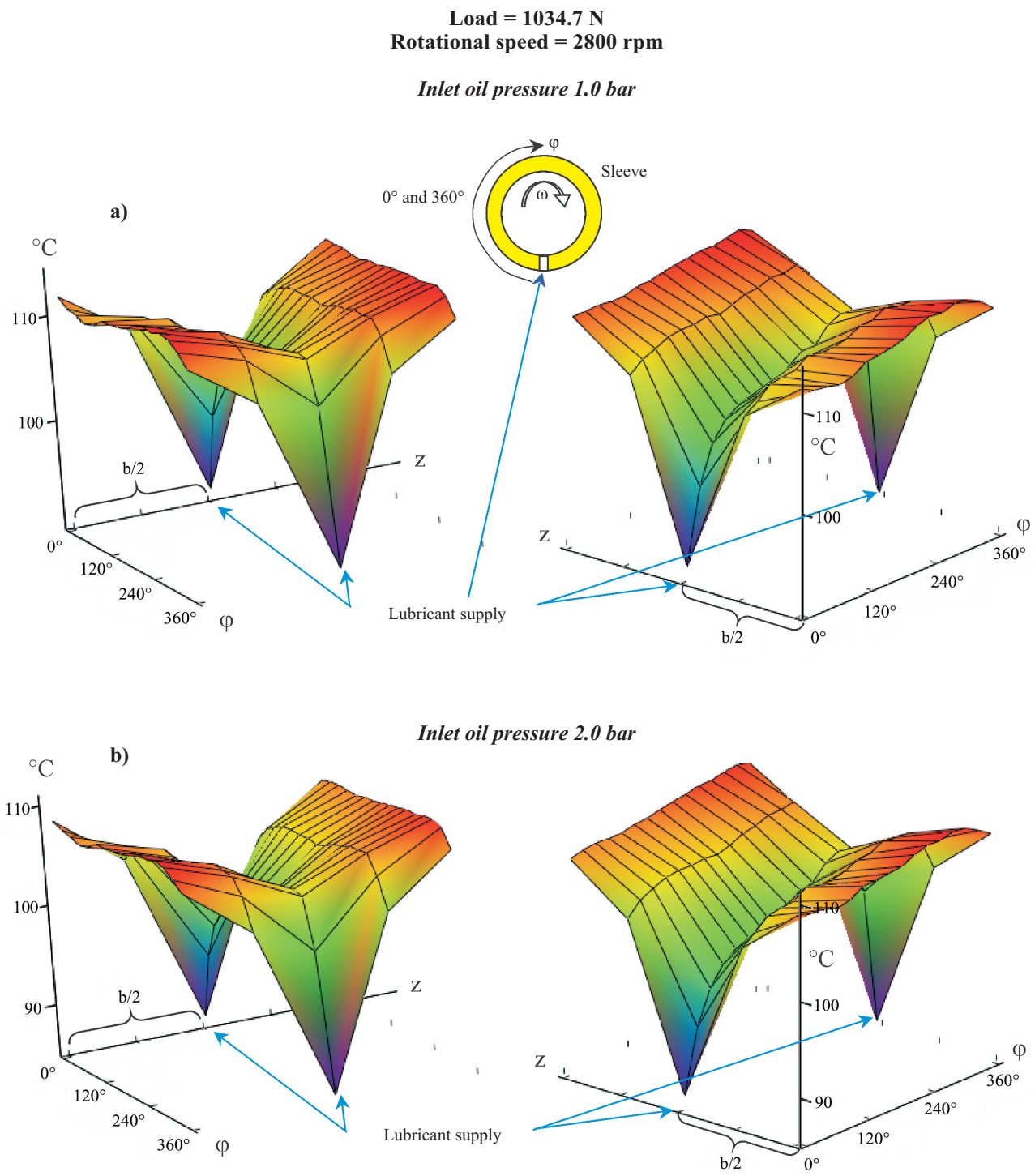

Fig. 6. *Distributions of the temperature measured on the sleeve under 1034.7 N load and 2800 rpm rotational speed of the journal, for 70°C temperature of oil at inlet, and the different values of the oil pressure*

Results for SAE 15W40 basic oil

During tests for the SAE 15W40 basic oil the sleeve was subjected to the same operational conditions as those for the tests of the preceding oils. The relevant results of temperature distributions are shown in Fig.7 and 8.

Load = 1034.7 N Inlet oil pressure = 1.5 bar

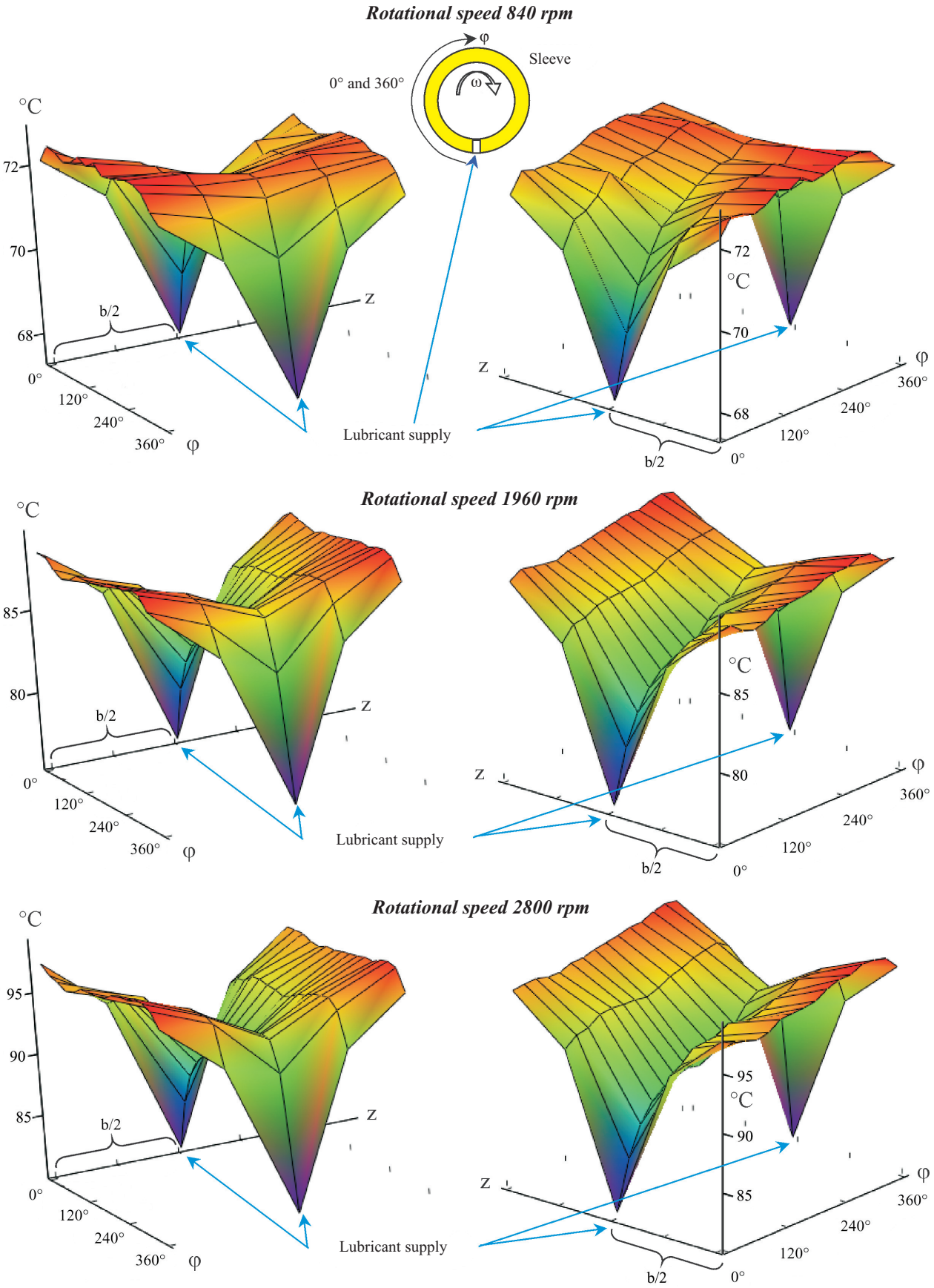

Fig. 7. Distributions of the temperature measured on the sleeve under 1034.7 N load at 1.5 bar pressure and 70°C temperature of oil at inlet, and the different values of journal's rotational speed

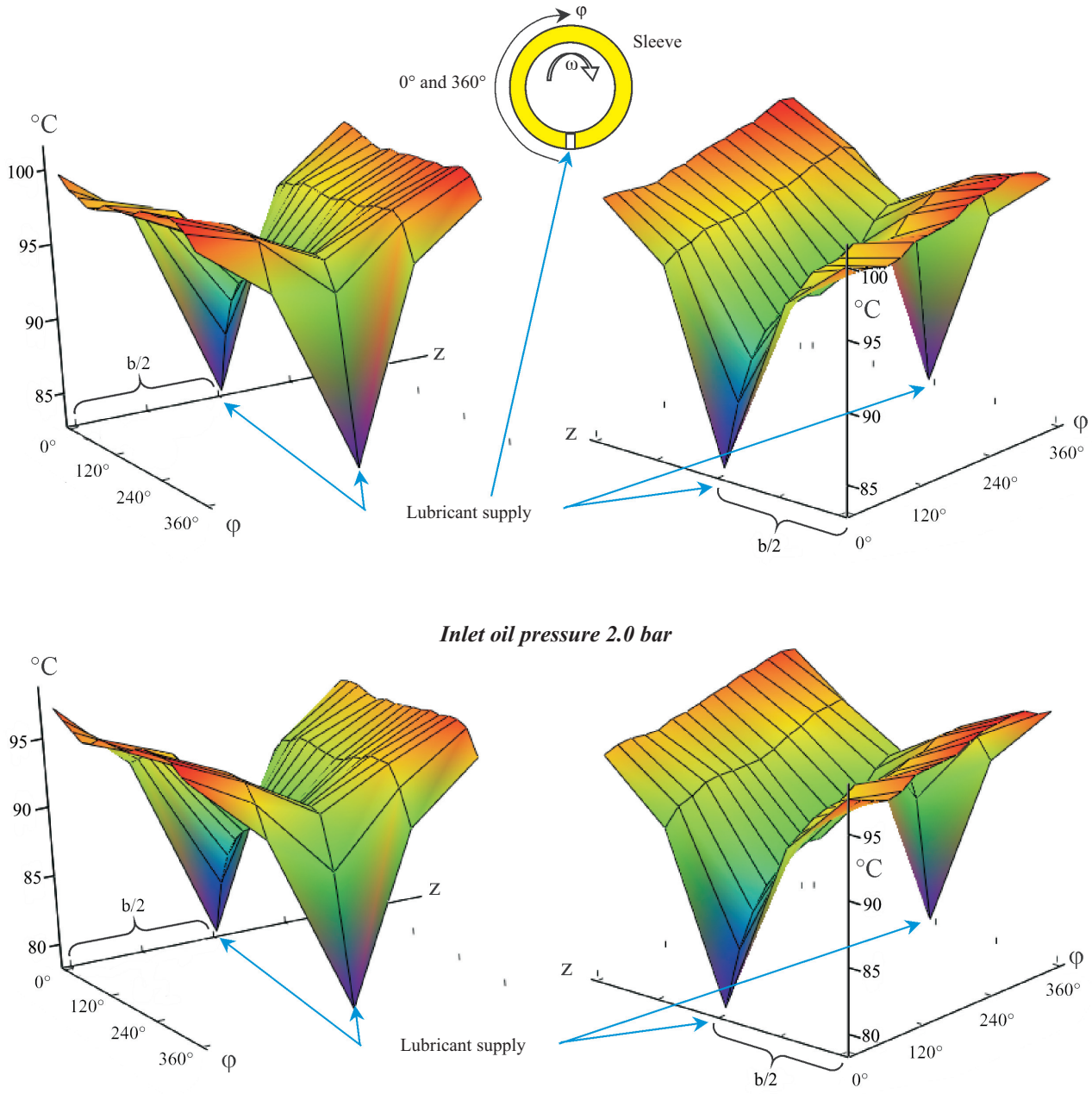

Fig. 8. *Distributions of the temperature measured on the sleeve under 1034.7 N load and 2800 rpm rotational speed of the journal, for 70°C temperature of oil at inlet, and the different values of the inlet oil pressure*

Results for ferro-oil

The measured temperature distributions concerned possible changes resulting from changes of journal's rotational speed and simultaneous action of magnetic field induction at a given load exerted on the bearing. Three first figures present the temperature distribution for rotational speeds of : 840 rpm; 1960 rpm; and 2800 rpm under 1034.7 N load on the sleeve and no external magnetic induction field.

The measured values presented in Fig.10 were obtained for the same speeds, inlet oil pressure and load, but for the magnetic induction field of about 30 mT intensity.

Fig.11 presents the temperature distributions also for the same rotational speeds, 1034.7 N load and 1.5 bar inlet oil pressure, but for the magnetic induction field of about 55 mT intensity.

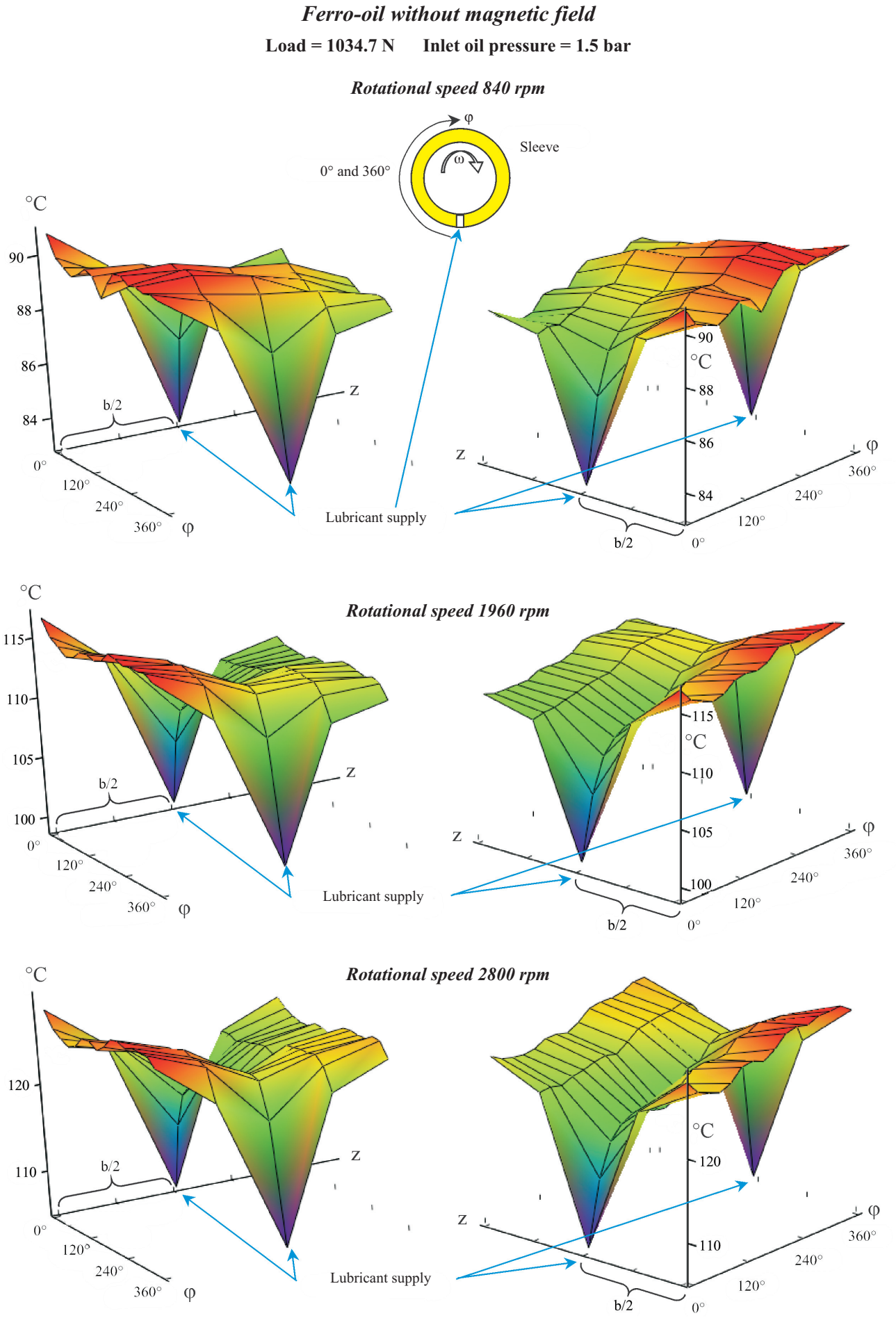

Fig. 9. Distributions of the temperature measured on the sleeve under 1034.7 N load at 1.5 bar pressure and 70°C temperature of oil at inlet, and the different values of journal's rotational speed (no magnetic induction field)

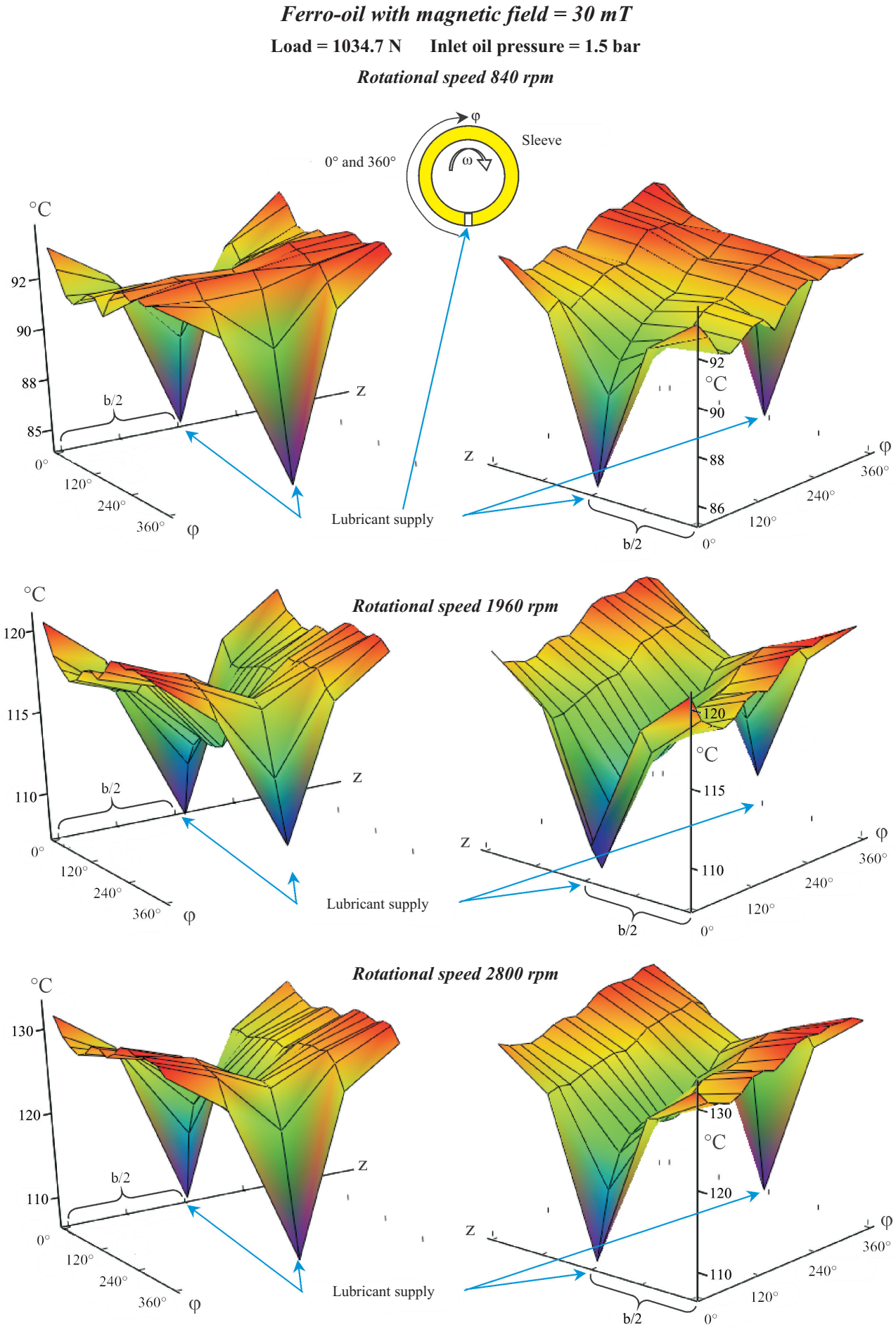

Fig. 10. Distributions of the temperature measured on the sleeve under 1034.7N load at 1.5 bar pressure and 70°C temperature of oil at inlet, and the different values of journal's rotational speed (under magnetic induction field of 30 mT)

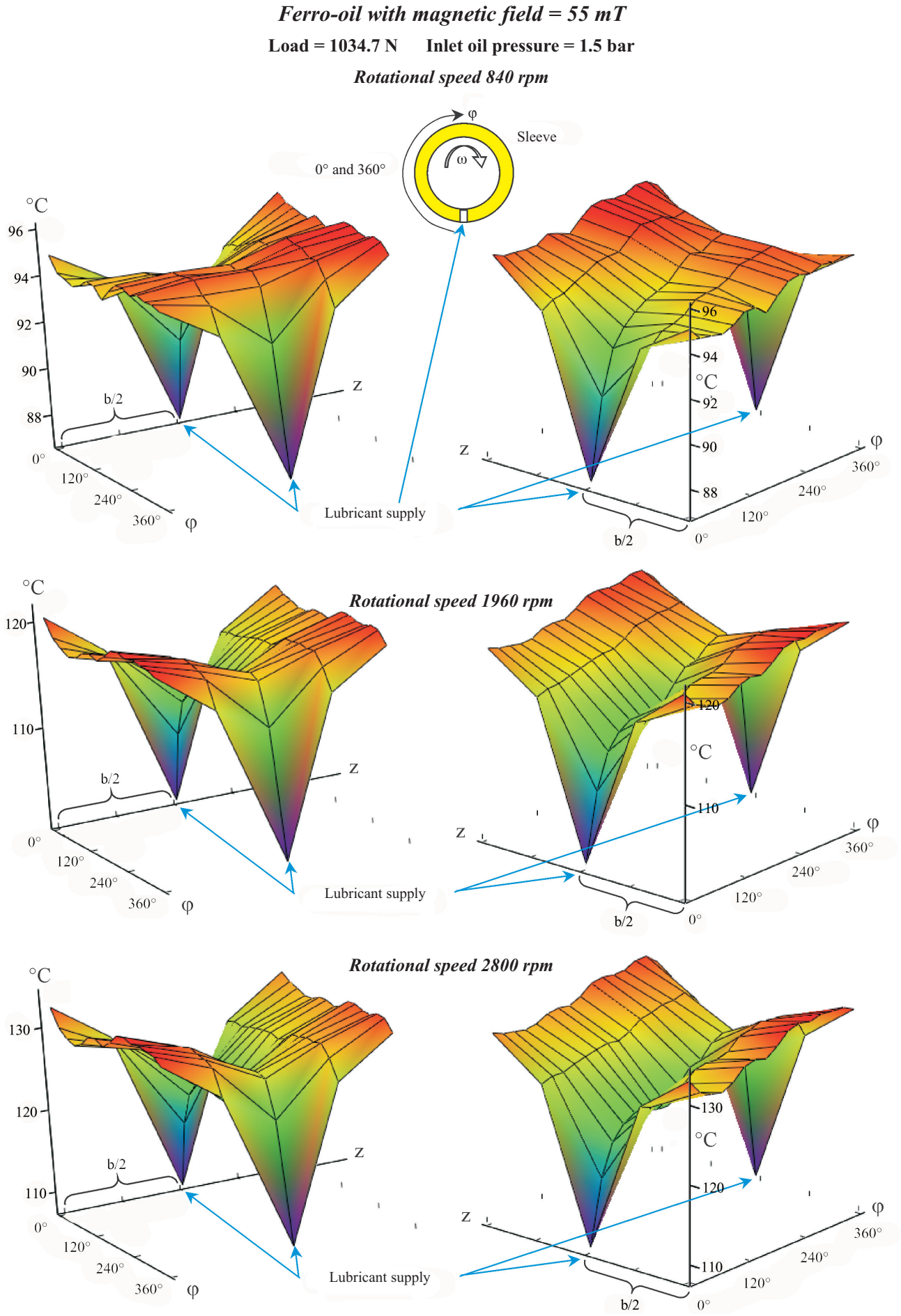

Fig. 11. Distributions of the temperature measured on the sleeve under 1034.7N load at 1.5 bar pressure and 70°C temperature of oil at inlet, and the different values of journal's rotational speed (under magnetic induction field of 55 mT)

DISCUSSION OF THE TEST RESULTS

- Apart from the above presented results of temperature measurements also the Delo®1000 Marine 30 waste oil was investigated. The obtained results differed only slightly from those for the fresh oil of the same grade. Because of publishing limitations, results of temperature measurements for the remaining oils and other operational parameters, (e.g. for 2020 N load) are not included in this paper, nevertheless they have been analyzed and discussed.
- Analyzing the values of temperature distribution one can state that the distributions for the fresh oil and waste one for the same operational parameters of the bearing differ only slightly.
- The rotational speed influence on the change of temperature distribution in the Delo®1000 Marine 30 fresh oil, at 1034.7N load, amounts to about 26% for the increase of journal's rotational speed from 840 rpm to 1960 rpm, and for the increase from 840 rpm to 2800 rpm – to about 39%.
- In the case of the waste oil at 1034.7N load on the bearing the rotational speed changes influence on the change of temperature distribution amounts to about 24% for the increase of journal's rotational speed from 840 rpm to 1960 rpm, and to about 41% for the increase from 840 rpm to 2800 rpm.
- In the case when the bearing is loaded with 2020N load, the influence of rotational speed on change of temperature distribution in the fresh Delo®1000 Marine 30 oil amounts to about 23% for the increase of journal's rotational speed from 840 rpm to 1960 rpm and to about 35% for the increase from 840 rpm to 2800 rpm.
- In the case of the Delo®1000 Marine 30 waste oil and for 2020N load exerted on the bearing the rotational speed influence on change of temperature distribution amounts to about 24% for the increase of journal's rotational speed from 840 rpm to 1960 rpm, and to about 37% for the increase from 840 rpm to 2800 rpm.
- The influence of inlet oil pressure on temperature distribution measured in the same points, both for the fresh and waste Delo®1000 Marine 30 oil at 1034.7N load on the sleeve, is slight. The inlet oil pressure increased from 1 bar to 1.5 bar lowers temperature values by about 3%, and by about 6% in the case when the oil pressure is changed from 1 bar to 2 bar. In the case when the sleeve is under 2020N load, the influence of inlet oil pressure on temperature distribution is negligibly smaller than that of inlet oil pressure on temperature distribution at a lower load.
- Analyzing the results of measured temperature distributions in the SAE 15W40 basic oil one can draw similar conclusions as those for the above discussed oil, however with the difference that the temperature values for all the just presented cases are by several percent lower than those obtained for the previously tested oil.
- Hence the influence of rotational speed on change of temperature distribution in the basic oil at 1034.7 N load amounts to about 23% for the increase of journal's rotational speed from 840 rpm to 1960 rpm, and to about 36% for the speed increase from 840 rpm to 2800 rpm.
- In the case when the bearing is under 2020 N load the rotational speed influence on change of temperature distribution in the SAE 15W40 basic oil amounts to about 20% for the increase of journal's speed from 840 rpm to 1960 rpm and about 30% for the speed increase from 840 rpm to 2800 rpm.
- The influence of inlet oil pressure on temperature distribution in the basic oil is also low. For 1034.7N load applied on the sleeve, and the same measurement points, it amounts to about 3.5% for the inlet oil pressure increased from 1 bar to 1.5 bar, and to 6.5% – when the pressure is changed from 1 bar to 2 bar.
- The influence of inlet oil pressure on temperature distribution in SAE 15W40 basic oil under 2020 N load exerted on the sleeve, measured in the same measurement points, is equal to about 2% for the inlet oil pressure increased from 1 bar to 1.5 bar, and 2.6% for the oil pressure increased from 1 bar to 2 bar, respectively.
- Analyzing the measured temperature distributions for ferro-oil, presented in Fig. 9÷11, one can draw similar conclusions as those for the previously considered oils, with the difference that the temperature values for all the cases actually considered are by a dozen or so percent greater than the temperature values obtained for the previously tested oils.
- When comparing temperatures of other oils with basic oil temperature it can be observed that the difference is even as great as 35%. Reminding that the ferro-oil was made of the basic oil, one can attribute its increased viscosity to the introduction of magnetic particles and the application of magnetic induction field.
- The influence of journal's rotational speed changes on temperature distribution changes during lubricating the bearing with the ferro-oil was tested for 1034.7N load exerted on the sleeve. When the journal's rotational speed was increased from 840 rpm to 1960 rpm the temperature increased by about 29% (at 0mT magnetic field intensity during measurements), 29% (at 30mT), 27% (at 55mT), and for the speed increase from 840 rpm to 2800 rpm the temperature increased by 43% (at 0mT), 42% (at 30mT), 40% (at 55mT) respectively.
- In the case when 2020N load was applied to the bearing the rotational speed influence on change of temperature distribution in the ferro-oil amounts to about 29% (at 0mT); 24% (at 30mT); 23% (at 55mT) as a result of the increase of journal's rotational speed from 840 rpm to 1960 rpm, and about 42% (at 0mT); 36% (at 30mT); 35% (at 55mT) as a result of the increase of journal's rotational speed from 840 rpm to 2800 rpm.
- The influence of inlet oil pressure on measured temperature distribution is, like for other oils, low and contained within the range of 2%÷3% as a result of the change of inlet oil pressure within the range of 1÷2 bar.

CONCLUSIONS

- Considering the obtained test results both presented and not presented in this paper (due to a huge amount of them) one can draw the following conclusions :
  - The difference between the values of temperature in the tested waste oil, distributed on the inner surface of the sliding bearing sleeve in question and those in the fresh oil of the same grade in the same lubricating conditions, is small. The temperature increase by a few percent for the waste oil can be justified by its increased viscosity. The greater viscosity makes values of friction force increasing and thus more heat is emitted. At the same amount of the flowing oil and a greater amount of heat generated within oil film its temperature must be higher than that of an oil of lower viscosity.

- Great differences can be observed between the distributions of temperature measured on the inner surface of the sliding bearing sleeve, for the ferro-oil and basic oil as well as those for the remaining tested oils, which can be justified by a difference in viscosity of the oils in question resulting from the presence of magnetic particles in the ferro-oil.
- By comparing the temperature distributions obtained for the basic oil with those for the ferro-oil affected by the magnetic induction field, at the load of about 1034.7N and the journal's rotational speed of 2800 rpm, the temperature increase by about 30÷40% can be stated on the inner surface of the sliding bearing sleeve.
- As the presented figures show, the rotational speed increase makes values of the sleeve's temperature increasing , as well as the difference between the highest and lowest value of sleeve's temperature greater. The high temperature drops appearing in the central part of the diagram result from the delivering of lubricating oil at 70°C temperature, to that point.
- The distinct temperature drop resulting from the increased load on the sliding bearing can be observed. The phenomenon could result from that at a high load the maximum lubricating gap increases, thus a greater amount of lubricating oil could flow through the gap at an assumed constant inlet oil pressure than that flowing through a narrower gap at a lower load.

- When analyzing the temperature distributions on the inner surface of the sliding bearing sleeve, are worth of noting the very great changes of temperature along the bearing length (a kind of „funnel" in the part of diagram corresponding with the central part of the bearing). The changes resulted from the way in which the oil was delivered : a flow of much cooler lubricating oil was point-wise delivered out of the lower part of the sliding sleeve to the lubricating gap in its greatest height. In this place it intensively cooled the journal and sleeve, due to which the temperature in the middle-length of the bearing from the side of oil delivery reached the lowest values.
- When analyzing the measured values of temperature distribution it can be observed that their circumferential changes reach a dozen or so degree centigrades depending on a journal rotational speed and load applied to sleeve.
- It should be remembered that the tested oils at the same radial clearance, load, rotational speed, inlet oil pressure and temperature could have various relative eccentricities resulting from different values of oil viscosity, which led to different heights of lubricating gap and different values of lubricant flow rate. The phenomenon also affected temperature distributions.

BIBLIOGRAPHY

1. Hebda M., Wachal A.: *Tribology* (in Polish). WNT (Scientific-Technical Publishing House). 1980
2. Korewa W., Zygmunt K.: *Essentials of machine construction* (in Polish) Part.I and II. WNT. Warszawa, 1971
3. Miszczak A., Wierzcholski K.: *Alterations introduced to T-05 test stand for measuring friction force in sliding bearing* (in Polish). 24th Autumn School on Tribology, Section of Exploitation of Machine, Mech. Eng. Committee, Polish Academy of Sciences. Krynica, 2000, Problemy Eksploatacji (Problems of Operation) No. 3/2000
4. Wierzcholski K., Miszczak A.: *Conversion of T-05 tester into a test stand for determining oil viscosity* (in Polish). Silesian University of Technology. Zeszyty Naukowe (Scientific Bulletins), No. 14/2000
5. Breczko T.: *Some aspects of calculation of transverse sliding bearings* (in Polish). Rozprawy Inżynierskie (Engineering Discourses), Vol. 23, No. 3/1975

CONTACT WITH THE AUTHOR

Andrzej Miszczak, D.Sc., M.E.
Gdynia Maritime University,
Faculty of Marine Engineering
Morska 81-87
81-225 Gdynia, POLAND
e-mail : miszczak@am.gdynia.pl

Miscellanea

TOP KORAB in 2004

Apart from its current activity, The Polish Society of Naval Architects and Marine Engineers, TOP KORAB every year arranges topical meetings dealing with shipbuilding and maritime economy.

In the year 2004, 12 such meetings had place :
9 in Gdańsk and 3 in Szczecin.

In Gdańsk the following topics were discussed :

- *New ship designs offerred by Gdynia Shipyard Co*
- *Building of replicas of ancient ships and boats in Europe*
- *Beginnings of ship model tests in Poland*
- *Diesel engines of MAN Co*
- *Beginning and development of Polish Register of Shipping*
- *Shipbuilding Secondary School in Warsaw in the years 1936 ÷ 1945*
- *Activity of Central Ship Design Office No.2*
- *Petrobaltic Co – a company exploiting hydrocarbon resources in Polish zone of Baltic Sea*
- *Flashback to 1958 ÷ 1980 : a balance of my professional career in Gdańsk Shipyard* (by K. Gniech).

And, the visiting trip to the Central Maritime Museum's branch house in Kąty Rybackie on the Vistula Sand Reef, was also organized.

The themes of the meetings in Szczecin were the following :

- *Reasons for downfall of Szczecin Shipyard Porta Holding Co*
- *LEADERSHIP 2015 – the plan of modernization of European shipbuilding and ship repair industry*
- *Selected problems of DNV activity aimed at improving safety at sea*.

Besides, the visit to GRYFIA Ship Repair Yard was arranged where the participants took part in a ship launching ceremony.

A new method for searching optimal path on a raster plane including cost of direction changes

Rafał Szłapczyński
Gdańsk University of Technology

ABSTRACT

The article introduces a new algorithm for finding optimal routes on raster planes. This method takes advantage of the new data structure and results in minimizing the number of direction changes within a route. It has linear time and space complexities and is sufficiently fast to perform real-time routing on the raster grids. Both the algorithm and its data structure are presented in detail in the paper. Possible applications of this method are also discussed.

Keywords : navigation, optimal route, turn penalties, Lee's algorithm, vave propagation, raster charts

1. INTRODUCTION

Raster grids are a digital representation of planary or spatial data, that is currently in use in many fields some of which belong to the maritime industry. Examples of application include pipeline and airduct design as well as navigational raster charts. Although the paper is focused on the navigational use of raster grids, its results may be easily adapted elsewhere.

The technology of electronic navigational charts (ENC) and digital electronic maps (DEM) has been used increasingly in maritime navigation, GPS and GIS systems [4]. As the raster charts are cheaper to be produced than vector ones they cover the majority of the electronic charts currently in use. In the ENC system one of the most common application is to determine an optimal route between a start cell and a destination cell, that does not cross any obstacles (landmass, barriers, shoals). The algorithm performing this should fulfill certain conditions. Of these the most obvious is that it does indeed find an optimal route if only such exists. Other conditions are those of needed time and memory space. In reality only algorithms of linear time and space complexities are useful as only such may be accepted by a real-time system processing large numbers of cells. The big *O* notation is further used for complexities, with *O(n)* indicating linear complexity [2].

The first solution to meet the above mentioned conditions was the maze routing algorithm presented by Lee [3], often described as a wave propagation process. To date, Lee's algorithm and its variations are among the most widely used routing methods finding applications in maze games, VLSI design and road map routing problems. However, the original algorithm proposed by Lee has one serious drawback: it works only for the 2-geometry grid plane (also known as the Manhattan geometry). Only recently it has been upgraded to higher geometries while sustaining the linear time and space complexities. This new solution has been proposed by Chang, Jan and Parberry [1].

Despite the major progress, the potential use of the improved Lee's algorithm has still some limitations. Both the original algorithm and its upgraded version tend to find the shortest path which is not always identical to the optimal one. In presence of many obstacles the algorithms determine a route containing so many turning points and course alterations that no navigator would be able to follow it even being so advised by a real-time routing system. Furthermore over larger geographic areas both distance and number of turns will contribute to the total time spent traversing a tour. Thus minimizing the number of turns is a desirable objective. Although the Chang, Jan and Parberry algorithm may cover the aspect of varied terrain (among other improvements) its data structure, based on that of the original Lee's method, makes it unable to include the cost of a turn in path length.

There is a number of methods (invented mostly for VLSI and automation purposes) that cover the problems of minimum bend path and shortest minimum bend path. Unfortunately, determining the shortest minimum bend path is of no value for long distance sea routing. Instead, the objective is finding the shortest paths with bend penalizing. The bend penalizing issue has been also considered in a number of works but the methods presented there are either not sufficiently fast or not applicable for higher geometries.

The article proposes a solution to this problem. A new data structure has been so designed as to reflect the cost of all course alterations in each cell's arrival time. An algorithm utilizing such structure has been implemented. The algorithm uses the following input parameters: user specified values of the costs of time of course alterations (turn penalties). It returns the determined path.

In Sec. 2 the original Lee's method and its version upgraded by Chang, Jan and Parberry are described in detail. Sec. 3 presents a new algorithm that overcomes their limitations. In Sec. 4 some possible applications of this new solution are discussed, and finally the conclusions are presented.

2. THE MAZE ROUTING ALGORITHM : PAST SOLUTIONS

To facilitate checking out the Chang, Jan and Parberry version of the routing method its original notation is used here. In Sec. 3 the same notation is also used for the description of the new solution.

Lee's algorithm for the 2-geometry grid plane

The popularity of this method lies in its simplicity and the guarantee to find the shortest path if only such exists. Since it is widely known no formal description is given here.

Data structure

The cell map static data is stored in an array containing two fields for every cell :

SL – Boolean field whose value indicates whether a cell is assigned to sea or landmass (or any other static obstacle). *True* for sea, and *false* otherwise.

AT – Integer number field whose value is this cell arrival time, i.e. time needed to travel from the source cell to this cell.

The dynamic data are stored in two lists : L_1 and L_2 containing cell pointers or indexes in the cell array.

Algorithm overview

A cell array is initialized with appropriate *SL* and *AT* values. Two lists L_1 and L_2 are defined to keep track of the cells on the front of the wave (frontier cells) and their equal-distance-step neighbouring cells, respectively. Putting the source cell in the list L_1 initializes the search. After all neighbouring cells of L_1 are included into the list L_2, the list L_2 is processed, so that an expanded wave front is found. Then every cell of L_1 is deleted if all of its neighbouring cells are processed (updated) and L_1 is updated by this new front of the wave. The search is terminated when the destination cell is found or – in the case of the barrier of obstacles – there are no more new cells to be processed, i.e. the last front of the wave has not generated any neighbouring obstacle-free cells.

The Lee's algorithm version upgraded by Chang, Jan and Parberry

This method expands 2-geometry routing to any higher geometry. Details for an example 4-geometry routing are presented beneath. Varied terrain aspect is not considered here as it increases the number of necessary lists, though it is generally supported by this version.

2-geometry and 4-geometry movement rules

Possible moves from a cell on the 2-geometry and 4-geometry grid planes are shown on the diagrams below.

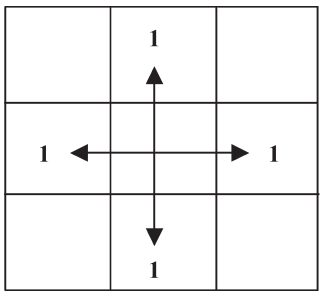

Fig.1. A 2-geometry neighbourhood

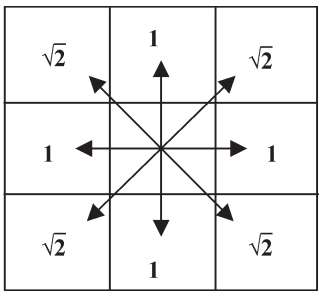

Fig.2. A 4-geometry neighbourhood

Data structure

The static data is stored in an array containing three fields for every cell :

SL – Integer number field whose value indicates whether a cell is assigned to sea or landmass (or any other static obstacle). Its value is 1 for sea, and infinity for a landmass.

AT – Floating point number field whose value is this cell arrival time – time needed to travel from the source cell to this cell.

VIS – Boolean field whose value indicates whether a cell has been already visited (inserted to *temp-list*) or not. *True* for a visited cell, *false* otherwise.

The dynamic data is stored in three circularly used lists: L_1, L_2, L_3 and one temporary list (*temp-list*). The index of a list currently in use is stored in a *bucket_index* variable. All lists contain cell pointers or indexes in the cell array.

Algorithm overview

There are some major differences between the 2 - and 4-geometry algorithms. Firstly, additional lists are introduced to control the propagation speed in different directions (the additional two diagonal directions have single-step distance equal to $\sqrt{2}$ instead of 1).

Secondly, the *VIS* cell field is introduced to make sure that each cell is inserted into temporary list exactly once. These two aspects make the algorithm keeping the original linear complexities.

Algorithm formal description

- The INSERT procedure inserts the index of c_i into the *temp-list*.
- The procedure CLEAR empties any given list.
- The RETRACE procedure retraces from the destination cell to the source cell according to their smallest *AT* value and builds a path LL_{path} which is the output of the 4-geometry maze router.

Algorithm (in Pascal) of 4-GEOMETRY-ROUTER (*Cell-map*, *S*, *D*, LL_{path})

```
Input: Cell-map, S, D
Output: LL_path
begin
 bucket_index : = 0 ;
 L_bucket_index : = S ;
 VIS_s : = TRUE ;
 temp-list : = Ø ;
 path-exists : = FALSE ;
 while (L_bucket_index ≠ Ø) or (L_bucket_index+1 ≠ Ø) do
  if (D cell in L_bucket_index) then
    begin
     path-exists : = TRUE ;
     break while ;
    end
  for each cell c_i in L_bucket_index do
    begin
     for each cell c_j neighbouring c_i do
       begin
        if (SL_j = 1) then
          begin
           if (VIS_j = FALSE) then
             begin
              VIS_j : = TRUE ;
              INSERT(c_j , temp-list) ;
             end
           Case 1: 2-geometry neighbours
            AT_new : = AT_i + 1 ;
           Case 2: diagonal neighbours
            AT_new : = AT_i + √2 ;
           if (AT_new < AT_j) then AT_j : = AT_new ;
          end
       end
    end
```

```
   CLEAR(L_bucket_index)
   if (temp-list ≠ Ø) then
    begin
     for each cell c_j in temp-list do
      INSERT(c_j , L_floor (Atj) mod 3)
     CLEAR (temp-list) ;
    end
   else bucket_index : = (bucket_index + 1) mod 3 ;
  end while ;
  if (path-exists = TRUE) then
   RETRACE(Cell-map(AT_D) , LL_path)
  else path does not exist ;
end .
```

3. PRESENTATION OF THE NEW SOLUTION

To simplify the presentation only the 4-geometry version is described here. However in general the algorithm is applicable to all geometries and it may also support varied terrain routing just the way the Chang, Jan and Parberry version does.

Data structure

The static data is stored in an array containing three fields for every cell :

SL – Integer number field whose value indicates whether a cell is assigned to sea or landmass (or any other static obstacle). Its value is 1 for sea, and infinity for a landmass.

GAT – A sub-array of the floating point numbers. The size of the array is equal to the maximum number of the neighbouring cells and is 8 for 4-geometry. Each field of this sub-array contains the gate arrival times for different incoming gates of the current cell. Gate arrival time is the time taken to travel from the source cell to the current cell via certain neighbour of the current cell.

VIS – Boolean field whose value indicates whether a cell has already been visited (inserted to *temp-list*) or not. *True* for a visited cell, *false* otherwise.

The dynamic data is stored in circularly used lists: $L_1 \ldots L_n$, and one extra temporary list *temp-list*. The number *n* of the used lists strictly depends on the specified maximum course alteration cost and thus it is indirectly configured by means of algorithm input parameters. *n = ceiling(maximum{single-step distances} + maximum{specified course alteration costs} + 1)*, where : *maximum(single-step distances)* is $\sqrt{2}$ for 4-geometry.

Algorithm overview

The key difference between the new solution and that proposed by Chang, Jan and Parberry is a replacement of each cell's *AT* field with *GAT* array. The idea of incoming gates arrival times makes it possible to take into account course alteration costs without sacrifying the linear complexities that characterized the previous versions. Every time cell data is updated, the arrival time of the appropriate gate is modified depending on the direction of the neighbouring cell that has initiated the update operation. The new candidate value of the gate arrival time field is determined according to the following formula :

$$GAT_{new,\,j,\,gate\_number} = \text{minimum}\ \{GAT_{i,1} + \\ + \text{distance}_{i\,,\,j} + \text{delay}_{gate\_number,1}, \ldots\ GAT_{i,8} + \\ + \text{distance}_{i\,,\,j} + \text{delay}_{gate\_number,8}\},$$

where :

i and *j* are indexes of the neighboring cells,
gate_number is the current gate of the c_j cell ,
numbers from 1 to 8 denote all gates of the c_i cell.

Delay values (penalties) are equal to zero for two gates of the same direction and have appropriate parameter values: d_1, d_2 or d_3 for two gates whose direction difference is 45°, 90° or 135°, respectively. The present *GAT* value is replaced with the candidate value if the new value is lesser than the current one.

The below presented diagrams illustrate the way the *GAT* array values of the wave front cells are updated.

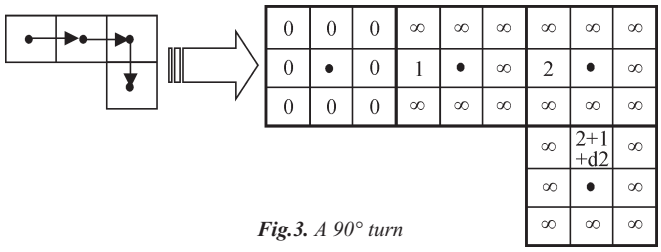

Fig.3. A 90° turn

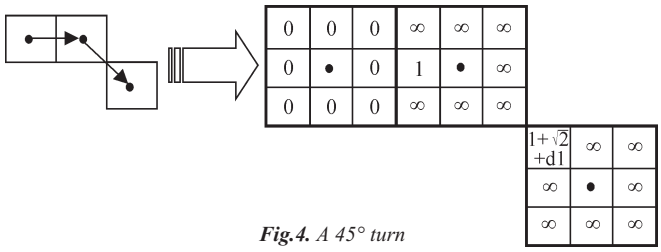

Fig.4. A 45° turn

Algorithm formal description

★ The procedures INSERT and CLEAR perform the same functions as those in the Chang, Jan and Parberry method.

★ The function GET_GATE_NUMBER (c_i,c_j) returns the number of the incoming gate of the cell c_j , through which the travel from the cell c_i is performed.

★ The procedure RETRACE retraces from the destination cell to the source cell and forms the output LL_{path} list. However, the rule of choosing the back way cells is different from that of the Chang, Jan and Parberry procedure. Here is chosen the cell whose sum of d_i ($i \in \{1,2,3\}$) modifier and the arrival time value of previous (closer to destination) cell's incoming gate is minimum.

Algorithm (in Pascal) of 4-GEOMETRY-ROUTER-WITH--TURN-PENALTIES (*Cell-map*, *S*, *D*, d_1, d_2, d_3, LL_{path})

```
Input: Cell-map, S, D, d_1 , d_2 , d_3
Output : LL_path
begin
 bucket_index : = 0 ;
 L_bucket_index : = S ;
 VIS_S : = TRUE ;
 temp-list : = Ø ;
 path-exists : = FALSE ;
 all-lists-empty : = FALSE ;
 number-of-lists : = ceiling(√2+ maximum{d_1 , d_2 , d_3}+1) ;
 while (all-lists-empty = FALSE) do
  if (D cell in L_bucket_index) then
   begin
    path-exists : = TRUE ;
    break while ;
   end
  for each cell c_i in L_bucket_index do
   begin
    for each cell c_j neighbouring c_i do
     begin
      if (SL_j = 1) then
       begin
        if (VIS_j = FALSE) then
         begin
```

```
            VIS_j : = TRUE ;
            INSERT(c_j , temp-list) ;
          end
        Case 1: 2-geometry neighbours
          distance : = 1 ;
        Case 2 : diagonal neighbours
          distance : = √2 ;
        gate_number : = GET_GATE_NUMBER(c_i,c_j) ;
        GAT_new : = GAT_i , gate_number + distance ;
        for each gate g_k of the cell c_i do
          begin
            Case 1: gate_number is
            the same direction as g_k
              delay_k : = 0 ;
            Case 2: gate_number and
            g_k difference is 45 degrees
              delay_k : = d_1 ;
            Case 3 : gate_number and
            g_k difference is 90 degrees
              delay_k : = d_2 ;
            Case 4 : gate_number and
            g_k difference is 135 degrees
              delay_k : = d_3 ;
            GAT_new , k : = GAT_i , k +
            + distance + delay_k ;
            if (GAT_new , k < GAT_new) then
              GAT_new : = GAT_new , k ;
          end
        if (GAT_new < GAT_j , gate_number ) then
          GAT_j , gate_number : = GAT_new ;
      end
    end
  end
  CLEAR(L_bucket_index)
  if (temp-list ≠ Ø) then
    begin
      for each cell c_j in temp-list do
        begin
          k : = floor (minimum{GAT_j , 1 ,... GAT_j , 8}) mod
          number-of-lists ;
              INSERT (c_j , L_k) ;
        end
      CLEAR (temp-list) ;
    end
  else bucket_index : = (bucket_index + 1) mod
  number-of-lists ;
  all-lists-empty : = TRUE ;
  for each list L_i do
    begin
      if (L_i ≠ Ø) then
        begin
          all-lists-empty : = FALSE ;
          break for
        end
    end
  end while ;
  if (path-exists : = TRUE) then
  RETRACE(Cell-map(GAT_D) , LL_path)
  else path does not exist ;
end .
```

Computational complexity

For each cell c_i whose distance from the source cell is equal to or lesser than that of the destination cell, the following actions are performed :

- each of its neighbours c_j is checked and possibly updated
- for each of its neighbours c_j, each of the gates of the cell c_i is checked.

This gives the total of $(2\cdot\lambda)\cdot(2\cdot\lambda)\cdot n$ steps for the worst case, where λ is a constant denoting geometry level (eight neighbours and eight gates for 4-geometry) and n is the number of cells whose distance from the source cell is equal to or lesser than that of the destination cell. Thus the computational complexity of the proposed solution is $O(n)$.

Example results of application of the proposed routing method and the Chang, Jan and Parberry algorithm

Below example results for the new routing method and the Chang, Jan and Parberry algorithm are presented. It has been assumed that costs of direction changes are: 1, 2 and 3 for 45°, 90° and 135° degree turns, respectively.

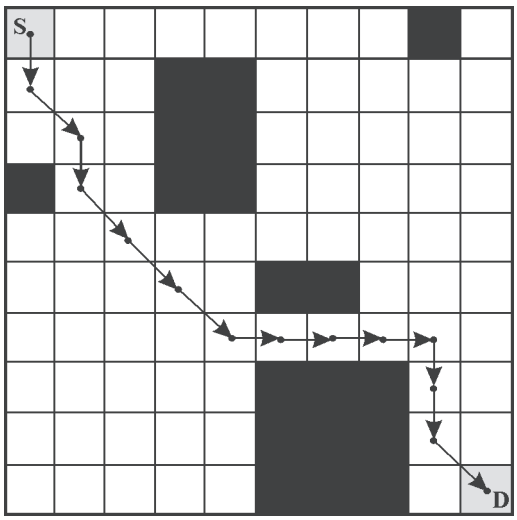

Fig.5. *Route determined by using the Chang, Jan and Parberry algorithm*

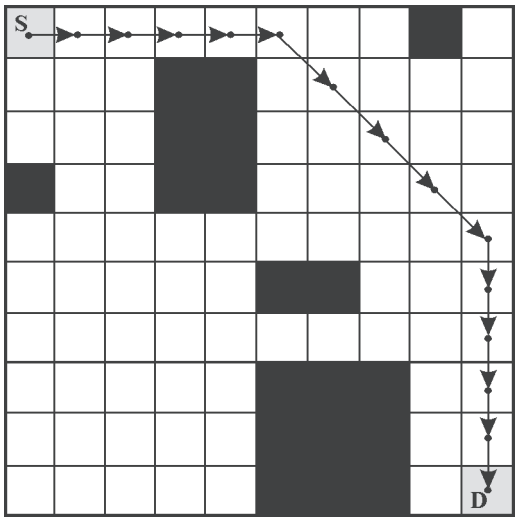

Fig.6. *Route determined by using the proposed algorithm with direction change costs (penalties) $d_1 = 1$, $d_2 = 2$, $d_3 = 3$*

In the above presented figures two different solutions of the same task are compared. The proposed algorithm (Fig.6), found a route with two turning points, different from that yielded by the Chang, Jan and Parberry method (Fig.5) which determined a route with six turning points. Thus the total path lengths and penalties for both methods are :

For the route by the Chang, Jan and Parberry method :

basic path length = $8 + 5\cdot\sqrt{2} \approx 15.07$

total penalties = $5\cdot d_1 + 1\cdot d_2 = 7$

total path cost = basic path length + total penalties ≈ 22.07

For the route by the proposed method :

$$\text{basic path length} = 10 + 4\cdot\sqrt{2} \approx 15.65$$
$$\text{total penalties} = 2\cdot d_1 = 2$$
$$\text{total path cost} = \text{basic path length} + \text{total penalties} \approx 17.65$$

From this comparison it can be stated that taking a seemingly longer (by 3.8%) route results in a much lower (by 22%) overall path cost.

4. EXAMPLES OF APPLICATION

The algorithm described in the paper is of general use. Therefore, whenever routing on the grid is involved and costs of direction changes matter, the benefits of using the proposed solution may be considerable.

In navigation, real-time routing and collision avoidance systems are the most obvious fields where the algorithm may be adapted. The method is applicable for ENC systems and ECDIS display on raster plane in particular. For a detailed description of a routing with collision avoidance system that may take advantage of the presented algorithm, the reader is referred to the paper [1].

Other potential maritime applications include pipeline and airduct routing, where minimizing the number of bends is crucial for cutting down the costs. However the algorithm would have to be first upgraded to a 3-D version. Fields of use outside maritime industry may include VLSI design.

5. SUMMARY

In the paper a general searching method on the raster plane was presented. Owing to its new data structure the algorithm is capable of including costs of direction changes in the total cost of an optimal path, while keeping the linear computational time and space complexities. Therefore when costs of direction changes are significant the solution is superior to those previously known. Possible applications include finding optimal ship routes since their course alterations might be expensive or even risky in presence of obstacles.

NOMENCLATURE

List of variables used in the algorithms :

all-lists-empty	– indicates whether all buckets (lists) are empty or not
AT_{index}	– the arrival time (a time when the cell of the given index can be reached)
bucket_index	– index of the bucket currently in use
Cell-map	– a map of cells, containing all relevant information
d_1 , d_2 , d_3	– the turn penalties (delay times for 45, 90 and 135-degree turns, respectively)
delay	– a delay resulting from the direction change
distance	– the distance between two neighbouring cells
D	– a destination cell
gate_number	– the number of the incoming gate, through which the cell is reached
$GAT_{cell\_index,\ gate\_number}$	– the gate arrival time (a time when the incoming gate of the given cell can be reached)
LL_{path}	– the returned path
number-of-lists	– the number of the buckets (implemented as lists)
path-exists	– indicates whether the searched path has been found or not
S	– a start cell
SL_{index}	– indicates whether the cell of the given index is sea (passable) or land (impassable)
temp-list	– a temporary list
VIS	– indicates whether a cell of the given index has already been visited
∅	– empty list

Abbreviations

DEM	– Digital Electronic Maps
ECDIS	– Electronic Chart Display and Information System
ENC	– Electronic Navigational Charts
GIS	– Geographical Information System
GPS	– Global Positioning System
VLSI	– Very Large Scale Integration
2- and 4-geometry	– two, four trajectories, respectively
3-D	– three dimensions

BIBLIOGRAPHY

1. Chang K. Y., Jan G.E, Parberry I. : *A Method for Searching Optimal Routes with Collision Avoidance on Raster Charts*. Royal Institute of Navigation. The Journal of Navigation No.56/2003
2. Kubale M. : *Introduction to Computational Complexity*. Wydawnictwo Politechniki Gdańskiej (Publishing House of Gdańsk University of Technology). 1994
3. Lee C.Y. : *An Algorithm for Path Connection and Its Applications*. IEEE (Institute of Electrical and Electronics Engineers) Transactions on Electronic Computers, EC-10, 1961
4. Weintrit A. : *The Electronic Chart Systems and Their Classification*. Annual of Navigation, No 3/2001. Polish Academy of Sciences. Polish Navigation Forum, Gdynia 2001

CONTACT WITH THE AUTHOR

Rafał Szłapczyński, M.Sc.,Eng.
Faculty of Ocean Engineering
and Ship Technology,
Gdańsk University of Technology
Narutowicza 11/12
80-952 Gdańsk, POLAND
e-mail : rafal@pg.gda.pl

Conference

SCIENTIFIC SEMINAR OF REGIONAL GROUP *of the Section on Exploitation Foundations*

On 25 November 2004 the Institute of Fluid-Flow Machinery, Polish Academy of Sciences (PAS), Gdańsk, hosted the last-in-the-year scientific seminar of the Regional Group of the Section on Exploitation Foundations, Machine Building Committee, PAS.

During the main part of the seminar 4 papers were presented whose authors came from scientific staff of the Institute, namely :

- *On energy and entropy* – by J. Mikielewicz
- *Plasma techniques applied to modern cars* by J. Mizeraczyk
- *Experimental modal analysis* – by M. Łuczak
- *Structural funds – research projects and their financial assembling* – by J. Kiciński

After interesting discussion on the papers Prof. J.Girtler, the Group's Chairman, presented a proposed plan of seminars for the year 2005.

The seminar was ended by presentation of the up-to-date laboratory facilities of the Institute.

FOREIGN *conference*

PSAM 7 – ESREL'04

On 14-18 June 2004 in Berlin had place the International Conference on :

Probabilistic Safety Assessment and Management

It was organized by two bodies : International Association for Probabilistic Safety Assessment and Management, and European Safety and Reliability Association.

Due to such arrangement its participants took part in a very broad meeeting of scientists, researchers and experts of many branches, which was demonstrated in 594 papers prepared by authors from 40 countries, from all the world around.

Among the gremium were also representatives of Polish scientific research centres who presented the following topics :

- ⇨ *Environmental safety of sea-going ship power plant* – by Brandowski A., and Liberacki R. (Gdańsk University of Technology)
- ⇨ *Risk in the aspect of safety and reliability of autonomous system* – by Drobiszewski J. and Smalko Z. (Warsaw University of Technology)
- ⇨ *New methods of solving multidimensional non-linear optimization problems – application thereof to construct air-line flight schedules* – by Jaźwiński J., Klimaszewski S., and Żurek Z. (Air Force Institute of Technology, Warsaw)
- ⇨ *Availability improvement of port transportation structures and their operation processes* – by Kołowrocki K. (Gdynia Maritime University)
- ⇨ *Incorporation of human and organizational factors into qualitative and quantitative risk analyses*- by Kosmowski K.T. (Gdańsk University of Technology)
- ⇨ *Modelling and uncertainty in system analysis for safety assessment* – by Kosmowski K.T. (Gdańsk University of Technology)
- ⇨ *On reliability improvement of the port grain transport systems* – by Kwiatuszewska – Sarnecka B. (Gdynia Maritime University)
- ⇨ *Reliability model of combined transportation system* by Nowakowski T. (Wrocław University of Technology).

Moreover, Mr J. Górski of Gdańsk University of Technology took part in the activity of *Application Area Co-ordinators*, a 16-person international organizational team, within the area : *Information Technology and Telecommunication*.

Miscellanea

World qualification level for welding engineers

Without doubt welding is one of the most important fields of engineering.

Welding, soldering and bonding – these are engineering processes which play an important role in production, repair and operation of objects. Therefore welding is teached in many engineering schools and universities worldwide.

However it has turned in practice that their graduates – – welding engineers with their qualification do not quarantee to cope with required responsible supervision over realized welding processes, which detrimentally influence quality and durability of produced engineering objects. In order to improve the situation European Federation for Welding (**EFW**) and International Institute of Welding (**IIW**) came to the conclusion that welding processes – from the point of view of quality assurance – require a.o. special surveillance by specially trained engineering personnel.

Education of such personnel is carried out during a special training supplementary to academic studies. It is realized in accordance with the requirements defined in guidelines for unified educational system (Minimum Requirements for Education, Examination and Qualification) issued by the above mentioned organizations. The requirements contain overall description of aims and scope of the education, as well as conditions and criteria for carrying out final examination to obtain the diploma of European/International Welding Engineer (EWE/IWE).

In Poland it was Gdańsk University of Technology which first undertook such a task, where at its Mechanical Faculty the IIW Approved Training Body was organized.

Its activity was initiated during spring semester of 2001/2002 academic year under the authority of Welding Institute, Gliwice, being the IIW Authorized National Body. The first 300-hour course of the education on the highest international level was completed in July 2004. All 24 participants of the course passed the very difficult final exam with the mean grade of "almost very good". This way they entered the group of welding engineers of the highest international level which makes it possible to take up the highest posts in this profession.